

Article

Serendipitous Identification of Azine Anticancer Agents Using a Privileged Scaffold Morphing Strategy

Silvia Cesarini ^{1,†}, Iliaria Vicenti ^{2,†}, Federica Poggialini ^{3,†}, Silvia Filippi ^{1,†}, Eleonora Mancin ¹, Lia Fiaschi ², Elisa De Marchi ¹, Federica Giammarino ², Chiara Vagaggini ³, Bruno Mattia Bizzarri ¹, Raffaele Saladino ¹, Elena Dreassi ³, Maurizio Zazzi ² and Lorenzo Botta ^{1,*}

¹ Department of Biological and Ecological Sciences, University of Viterbo, Via S.C. De Lellis s.n.c., 01100 Viterbo, Italy; c.cesarinisilvia@gmail.com (S.C.); silvia.filippi@unitus.it (S.F.); eleonora.mancin98@gmail.com (E.M.); elisa.demarchi@unitus.it (E.D.M.); bm.bizzarri@unitus.it (B.M.B.); saladino@unitus.it (R.S.)

² Department of Medical Biotechnologies, University of Siena, 53100 Siena, Italy; ilariavicenti@gmail.com (I.V.); lia.fiaschi@unisi.it (L.F.); federica.giammari@gmail.com (F.G.); maurizio.zazzi@gmail.com (M.Z.)

³ Department of Biotechnology, Chemistry, and Pharmacy (DBCF), University of Siena, 53100 Siena, Italy; poggialini5@student.unisi.it (F.P.); chiara.vagaggini@student.unisi.it (C.V.); elena.dreassi@unisi.it (E.D.)

* Correspondence: lorenzo.botta@unitus.it

† These authors contributed equally to this work.

Abstract: The use of privileged scaffolds as a starting point for the construction of libraries of bioactive compounds is a widely used strategy in drug discovery and development. Scaffold decoration, morphing and hopping are additional techniques that enable the modification of the chosen privileged framework and better explore the chemical space around it. In this study, two series of highly functionalized pyrimidine and pyridine derivatives were synthesized using a scaffold morphing approach consisting of triazine compounds obtained previously as antiviral agents. Newly synthesized azines were evaluated against lymphoma, hepatocarcinoma, and colon epithelial carcinoma cells, showing in five cases acceptable to good anticancer activity associated with low cytotoxicity on healthy fibroblasts. Finally, ADME in vitro studies were conducted on the best derivatives of the two series showing good passive permeability and resistance to metabolic degradation.

Keywords: privileged scaffold; triazines; pyrimidines; pyridines; scaffold morphing; anticancer activity



Citation: Cesarini, S.; Vicenti, I.; Poggialini, F.; Filippi, S.; Mancin, E.; Fiaschi, L.; De Marchi, E.; Giammarino, F.; Vagaggini, C.; Bizzarri, B.M.; et al. Serendipitous Identification of Azine Anticancer Agents Using a Privileged Scaffold Morphing Strategy. *Molecules* **2024**, *29*, 1452. <https://doi.org/10.3390/molecules29071452>

Academic Editor: M^o Ángeles Castro

Received: 15 February 2024

Revised: 11 March 2024

Accepted: 21 March 2024

Published: 24 March 2024



Copyright: © 2024 by the authors. Licensee MDPI, Basel, Switzerland. This article is an open access article distributed under the terms and conditions of the Creative Commons Attribution (CC BY) license (<https://creativecommons.org/licenses/by/4.0/>).

1. Introduction

The concept of the privileged scaffold was introduced by Evans in 1988 [1] and represents a molecular framework able to bind more than one receptor and act as agonist or antagonist, when conveniently functionalized. Among all the drug discovery strategies to harness privileged scaffolds, decoration with opportune substituents is a good technique that allows the exploration of the biologically relevant chemical space around the chosen promising framework [2]. In addition, scaffold morphing [3] and hopping [4] are useful procedures to replace the central core structure of an active molecule with the aim of identifying new bioactive entities with increased pharmacodynamic and pharmacokinetic properties.

Basic nuclei of great interest are azines, six membered aromatic heterocycles that contain at least one nitrogen atom. Therefore, triazines, pyrimidines and pyridines (Figure 1a), can be considered privileged scaffolds [5,6] since their high prevalence in commercially available drugs [7] and biologically relevant biomolecules (e.g., enzymes cofactors, nucleobases) [8].

In the last few years, our research group has been involved in the synthesis and decoration of privileged scaffolds [9]. Concerning triazines, our team recently published a paper [9] focused on the synthesis and evaluation of compounds 1–9 against severe

acute respiratory syndrome coronavirus type 2 (SARS-CoV-2) (Figure 1b). Unfortunately, from this library of molecules only compound 1 emerged as able to inhibit SARS-CoV-2 replication with an IC_{50} (half-maximal compound concentration inhibiting the 50% of virus replication) value of 12.1 micromolar (mM).

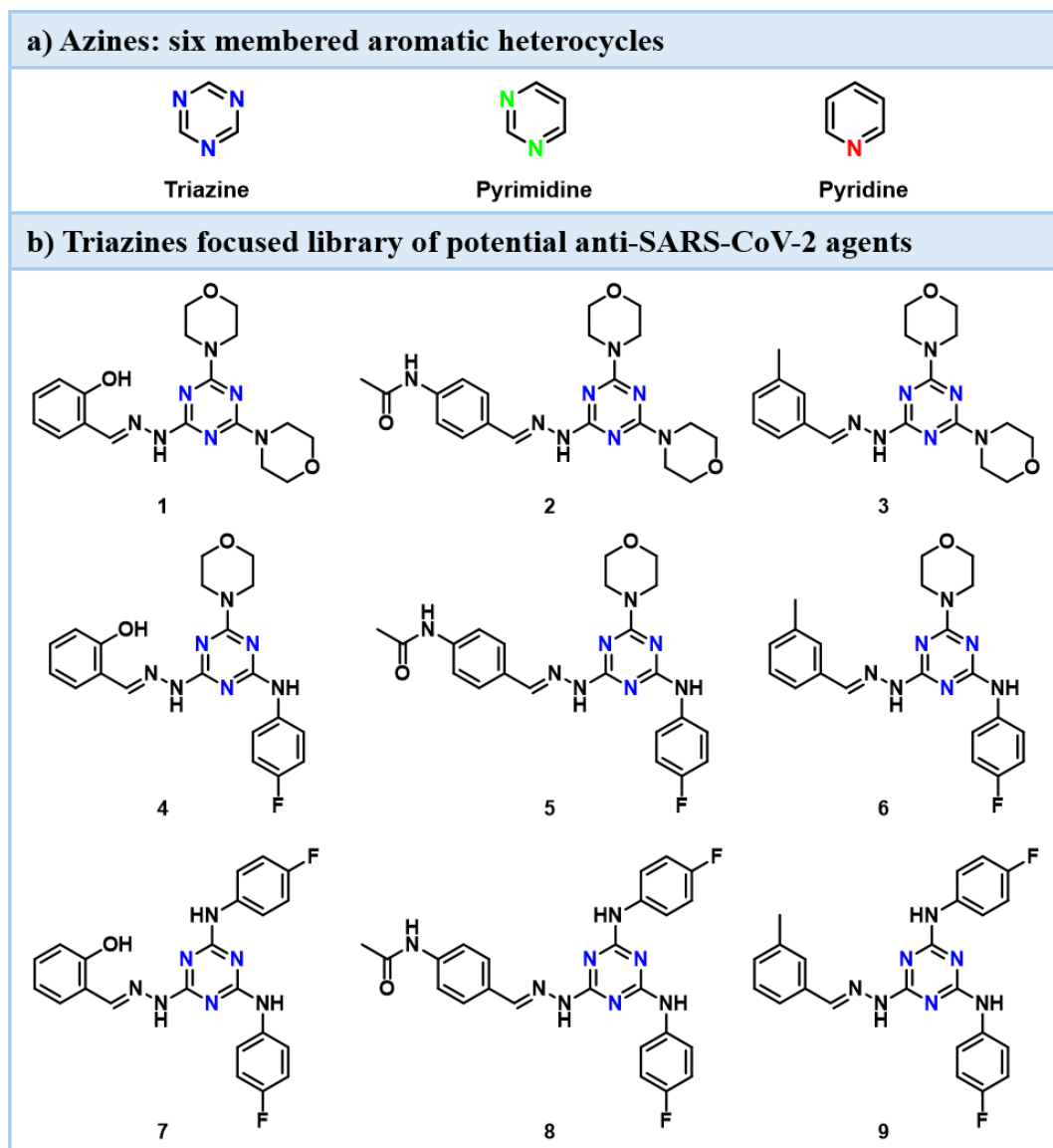


Figure 1. Chemical structure of three azine basic nuclei (a) and a focused library of triazine derivatives (1–9) synthesized in a previous work (b) [9].

Additional studies aimed at addressing a potential antiviral activity of derivatives 1–9 were conducted on several pathogens, highlighting a low or absent effect on human immunodeficiency (HIV-1), Dengue (DENV) and West Nile viruses (WNV). The exception registered was compound 4 that showed potency on flaviviruses DENV and WNV in the low micromolar range (2.0 and 1.1 μ M, respectively).

Surprisingly, viability assays conducted on uninfected lymphoma (H9), hepatocarcinoma (Huh7), and colon epithelial carcinoma (Caco-2) cells showed a cytotoxic effect of the synthesized molecules. This behavior prompts us to test compounds 1–9 on human normal fibroblasts FB789 and calculate the tumor selectivity indexes (TSIs) as the ratio between half-maximal compound cytotoxic concentration (CC_{50}) on FB789 and in turn CC_{50} in H9, Huh7 and Caco-2 (Table 1).

Table 1. In vitro cytotoxicity and tumor selectivity index (TSI) of the synthesized compounds in a cell-based model ¹.

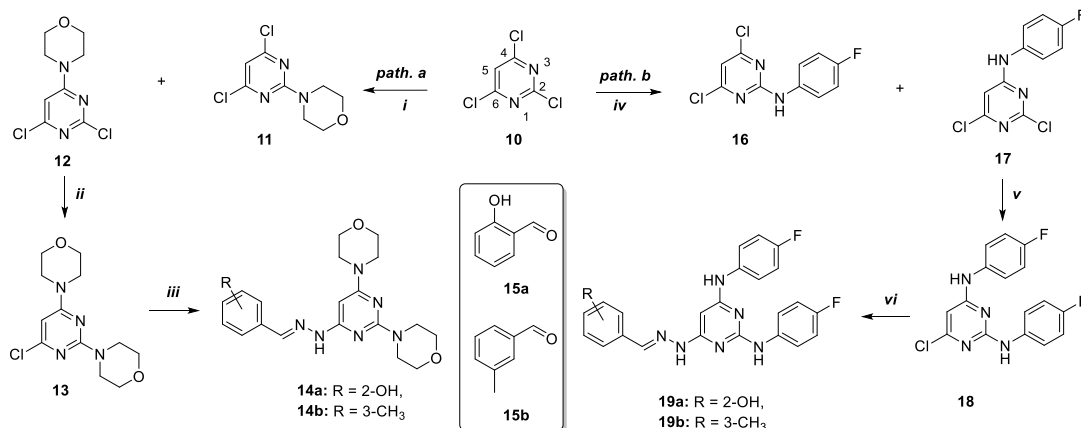
Entry	CPD	FB789 ²	H9 ²		Huh7 ²		Caco-2 ²	
		CC ₅₀ ³	CC ₅₀	TSI	CC ₅₀ μM	TSI	CC ₅₀	TSI
1	1	30 ± 6	>100	<0.3	>100	<0.3	>400	<0.1
2	2	134 ± 11	>100	<1.3	>200	<0.7	>200	<0.7
3	3	250 ± 10	74 ± 6.2	3.4	45 ± 10	5.6	184 ± 11	1.4
4	4	11 ± 3	2 ± 1	5.5	9 ± 1	1.2	3 ± 1	3.7
5	5	27 ± 3	30 ± 5	0.9	45 ± 6	0.6	70 ± 6	0.4
6	6	100 ± 8	>100	<1.0	47 ± 5	2.1	22 ± 2	4.5
7	7	7 ± 2	2 ± 1	3.5	2 ± 0.4	3.5	0.8 ± 0.1	8.8
8	8	57 ± 7	>100	<0.6	>200	<0.3	>200	<0.3
9	9	50 ± 5	>100	<0.5	>200	<0.2	200	0.2

¹ All experiments were conducted in duplicate in three independent experiments in FB789, H9, Huh7 and Caco-2 cells; ² experiment read-out 48 h; ³ CC₅₀, half-maximal compound cytotoxic concentration, expressed in micromolar (μM) range, as determined using Cell-Titer Glo kit (Promega, Madison, WI, USA). TSI, tumor selectivity index (ratio between CC₅₀ on FB789 and CC₅₀ on cancer cells H9, Huh7 and Caco-2). CPD = compound.

From all the evaluations made, derivatives **4** and **7** seemed to be interesting hit compounds, since they showed low micromolar antitumor activity on Huh7 (1.2 and 3.5 TSIs for derivatives **4** and **7**, respectively) and H9 (5.5 and 3.5 TSIs for triazines **4** and **7**, respectively) and a submicromolar effect on Caco-2 for compound **7** (8.8 TSI) (Table 1, entries 4 and 7). Moreover, from the cytotoxicity on FB789 cells point of view, triazine **3** highlighted the best profile compared to other compounds of the series (Table 1, entry 3). For these reasons, we decided to begin a study based on these results serendipitously obtained with triazine molecules aimed at the identification of potential antineoplastic agents for lymphoma, hepatocarcinoma and colorectal cancer. Hence, we decided to apply a scaffold morphing approach to replace the triazine core with pyrimidine and pyridine ones and to decorate these azine nuclei with the substituents that showed the best pharmacological performance in the previous study [9]. In detail, morpholine and 4-fluoroaniline were used as the pharmacophoric functionalities directly linked to the central six membered heterocycle. Salicyl and 3-methylphenyl hydrazones were chosen to complete the panel of substituents for the novel highly functionalized pyrimidine and pyridine products, since they are characteristic of the above-mentioned derivatives **3**, **4** and **7**. In the present study, two small libraries of a total twelve compounds were synthesized and were evaluated against H9, Huh7, and Caco-2 lines. Finally, the in vitro absorption, distribution, metabolism, and excretion (ADME) properties of selected derivatives were screened to define the most promising scaffold and the best highly functionalized derivative synthesized.

2. Results and Discussion

As depicted in Scheme 1 pathway a, highly functionalized trisubstituted pyrimidine derivatives **14a,b** were obtained in a three steps sequence starting from 2,4,6-trichloro pyrimidine **10** [10]. The latter was transformed into compounds **11** and **12** in 19 and 68% yield through reaction with morpholine in the presence of *N,N*-diisopropylethylamine (DIPEA) at 0 °C. The higher yield of the C6-substituted **12**, compared to the C-2 functionalized **11**, is due to steric hinderance exerted by the lone pairs of the N1 and N3 atoms that discourage the access of the nucleophile in the C2 position of the pyrimidine ring [11].



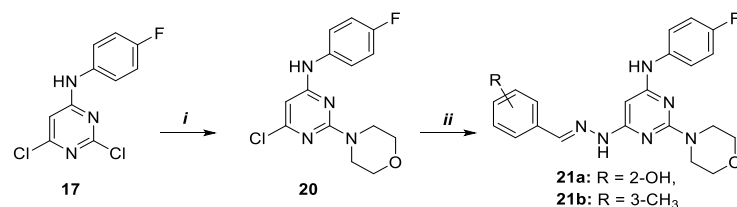
Scheme 1. Synthesis of pyrimidine derivatives **14a–b** (pathway a) and **19a–b** (pathway b). Reagents and conditions: (i) dichloromethane (CH₂Cl₂), morpholine, *N,N*-Diisopropylethylamine (DIPEA), 0 °C, 5 h; (ii) 1,4-dioxane, morpholine, HCl, MW, 110 °C, 40 min; (iii) 1. 1,4-dioxane, NH₂NH₂, MW, 100 °C, 4 h, 2. methanol (MeOH), **15a,b**, acetic acid, 25 °C, 24 h; (iv) CH₂Cl₂, 4-fluoroaniline, DIPEA, 0 °C, 5 h; (v) 1,4-dioxane, 4-fluoroaniline, HCl, MW, 110 °C, 40 min; (vi) 1. 1,4-dioxane, NH₂NH₂, MW, 100 °C, 4 h, 2. MeOH, **15a,b**, acetic acid, 25 °C, 48 h.

To distinguish between the two regioisomers, and for the final structure assignment, 2D NMR Nuclear Overhauser Effect Spectroscopy (NOESY) experiments were conducted [Supplementary Materials S1]. In derivative **12** it was possible to identify the interaction between the proton in position 5 of the pyrimidine ring and protons on the carbon atom adjacent to morpholine nitrogen, which was absent in **11**.

Then, **12** was subjected to a second substitution reaction always in the presence of morpholine at 110 °C under microwave (MW) irradiation to obtain Compound **13**. Finally, disubstituted pyrimidine **13** was reacted with hydrazine (NH₂NH₂) and subsequently with the opportune aldehyde, salicyl- and 3-methylphenyl-aldehydes **15a,b**, to give desired products **14a** and **14b** with 55 and 65% yield, respectively.

Highly functionalized pyrimidines **19a,b** were synthesized with a pathway similar to the above-described one (Scheme 1, path. b), using 4-fluoroaniline for the first two aromatic nucleophilic substitutions instead of morpholine.

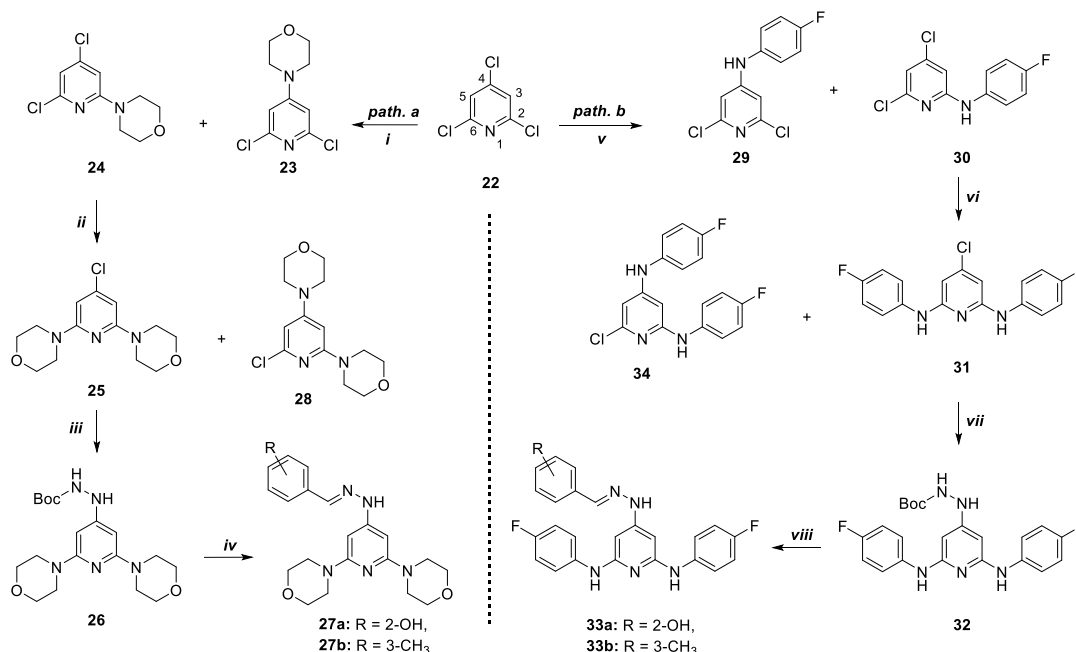
Pyrimidines **21a,b** were afforded starting from the monosubstituted intermediate **17** previously obtained (Scheme 2). The latter was easily turned into the final products through nucleophilic substitution with morpholine and the hydrazone two steps sequence installation.



Scheme 2. Synthesis of pyrimidine derivatives **21a,b**. Reagents and conditions: (i) ethanol (EtOH), morpholine, Et₃N, 80 °C, 18 h; (ii) 1. 1,4-dioxane, NH₂NH₂, MW, 100 °C, 6 h, 2. MeOH, **15a,b**, acetic acid, 25 °C 48 h.

Pyridine derivatives were synthesized as follows. Starting from 2,4,6-trichloropyridine **22**, through nucleophilic substitution with morpholine in tetrahydrofuran (THF) and triethyl amine (Et₃N) at 65 °C, a mixture of the two regioisomers **23** and **24**, bearing the amine substituent on C-4 and C-2, respectively, was obtained (Scheme 3, path. a). Structural assignment was made based on ¹H NMR experiments, being **23** symmetric and showing only one peak for C3–C5 protons in the recorded spectrum (Supplementary Materials S2).

From compound **24**, two regioisomeric pyridines, compounds **25** and **28**, were synthesized via morpholine nucleophilic substitution at 120 °C. Then, many attempts to directly introduce NH_2NH_2 on the heterocyclic ring were made, such as the use of high temperature, MW irradiation, and high concentration of NH_2NH_2 , but the desired pyridine carrying the hydrazine functionality on C-4 was never isolated. Finally, with tert-butoxy carbonyl (Boc) protected hydrazine, namely tert-butyl carbazate (BocNHNH_2), it was possible to decorate the C-4 position of the azine core [12]. When compound **26** was obtained, it was turned into the final trisubstituted products **27a,b** with 39 and 18% yield via acidic Boc removal in the presence of trifluoroacetic acid (TFA), and a reaction with the opportune aldehydes **15a,b** in a mixture of MeOH and a few drops of acetic acid at 25 °C.

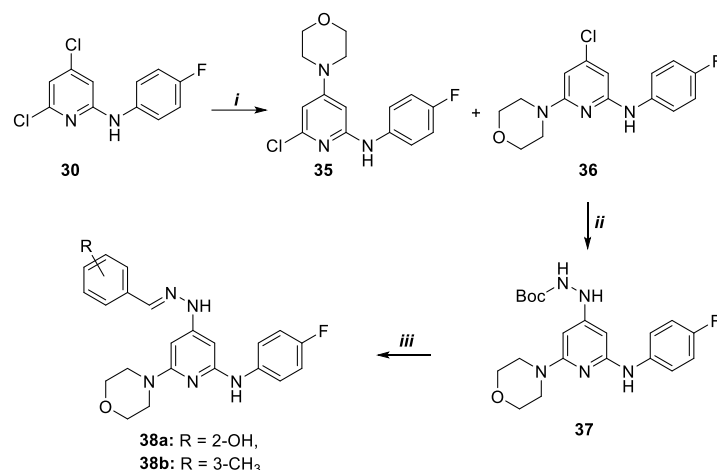


Scheme 3. Synthesis of pyridine derivatives **27a,b** (pathway a) and **33a,b** (pathway b). Reagents and conditions: (i) THF, morpholine, Et_3N , 65 °C, 18 h; (ii) dimethyl formamide (DMF), morpholine, DIPEA, 120 °C, 48 h; (iii) toluene, BocNHNH_2 , tris(dibenzylideneacetone)dipalladium (0) [$\text{Pd}_2(\text{dba})_3$], 1,1'-Bis(diphenylphosphino)ferrocene (DPPF), cesium carbonate (Cs_2CO_3), MW, 150 °C, 10 min; (iv) 1. CH_2Cl_2 , TFA, 25 °C, 1 h, 2. MeOH, **15a,b**, acetic acid, 25 °C, 24 h; (v) toluene, tetrakis(triphenylphosphine)-palladium (0) [$\text{Pd}(\text{PPh}_3)_4$], 4-fluoroaniline, Cs_2CO_3 , 150 °C, 24 h; (vi) toluene, palladium(II) acetate [$\text{Pd}(\text{OAc})_2$], 2,2'-Bis(diphenylphosphino)-1,1'-binaphyl (BINAP), 4-fluoroaniline, Cs_2CO_3 , 160 °C, 4 h; (vii) toluene, BocNHNH_2 , $\text{Pd}_2(\text{dba})_3$, DPPF, Cs_2CO_3 , MW, 150 °C, 10 min; (viii) 1. CH_2Cl_2 , TFA, 25 °C, 1 h, 2. MeOH, **15a,b**, acetic acid, 25 °C, 24 h.

With a similar route, the desired highly decorated pyridines **33a,b** were obtained (Scheme 3, path. B).

Finally, compounds **38a,b** were obtained in a 37% and 33% yield with a three step sequence starting from monosubstituted pyridine **30** (Scheme 4). The latter was converted into the desired products through reaction with morpholine at 160 °C, BocNHNH_2 insertion, deprotection and hydrazone formation in the presence of aldehydes **15a,b**.

All synthesized compounds were evaluated for their anticancer activity against lymphoma, hepatocarcinoma, and colon epithelial carcinoma on H9, Huh7 and Caco-2 cells, respectively (Table 2). Healthy FB789 fibroblasts were used as a reference for cytotoxicity determinations. TSIs were calculated as the ratio of CC_{50} values obtained with FB789 cells and, in turn, H9, Huh7 and Caco-2.



Scheme 4. Synthesis of pyridine derivatives **38a,b**. Reagents and conditions: (i) 1,4-dioxane, morpholine, DIPEA, 160 °C, 10 h; (ii) toluene, BocNHNH₂, Pd₂(dba)₃, DPPF, Cs₂CO₃ MW, 150 °C, 10 min; (iii) 1. CH₂Cl₂, TFA, 25 °C, 1 h, 2. MeOH, **15a,b**, acetic acid, 25 °C, 24 h.

Table 2. Cytotoxicity (μM) and antiproliferative activity (TSI) of highly functionalized pyrimidine and pyridine compounds against H9, Huh7 and Caco-2 cell lines ¹.

Entry	CPD	Ref. T. ³	FB789 ²		H9 ²		Huh7 ²		Caco-2 ²	
			CC ₅₀ ⁴	CC ₅₀ μM	TSI	CC ₅₀	TSI	CC ₅₀	TSI	
1	14a	1	30 ± 6	>100	<0.3	82 ± 6	0.4	84 ± 7	0.4	
2	14b	3	9 ± 1	14 ± 7	0.6	8 ± 4	1.1	11 ± 2	0.8	
3	19a	7	14 ± 3	31 ± 8	0.5	1 ± 0.3	14.0	2 ± 1	7.0	
4	19b	9	61 ± 9	48 ± 3.5	1.3	6 ± 1	10.2	4 ± 1	15.3	
5	21a	4	10 ± 5	11 ± 2	0.9	3 ± 1	3.3	2 ± 0.4	5.0	
6	21b	6	95 ± 1	>100	<1.0	67 ± 23	1.4	113 ± 4	0.8	
7	27a	1	11 ± 3	76 ± 4	0.1	44 ± 5	0.3	29 ± 2	0.4	
8	27b	3	81 ± 2	50 ± 4	1.6	39 ± 3	2.1	30 ± 2	2.7	
9	33a	7	0.3 ± 0.3	43 ± 9	0.01	18 ± 5	0.02	12 ± 4	0.03	
10	33b	9	390 ± 30	23 ± 7	17.0	21 ± 12	18.6	11 ± 9	35.5	
11	38a	4	3 ± 1	37 ± 2	0.1	24 ± 14	0.1	19 ± 0.1	0.2	
12	38b	6	90 ± 9	18 ± 4	5.0	9 ± 6	10.0	8 ± 3	11.3	

¹ Values are the means ± SD of experiments run in triplicate; ² experiments read out at 48 h; ³ Ref. T. = reference triazine, triazine derivative from which the newly synthesized pyrimidine or pyridine are derived; ⁴ CC₅₀, half-maximal compound cytotoxic concentration, expressed in micromolar (μM) units. TSI, tumor selectivity index (ratio between CC₅₀ on FB789 and CC₅₀ on cancer cells H9, Huh7 and Caco-2). CPD = compound.

In detail, cancer and normal cells were incubated in the presence of an increasing concentration of pyrimidine and pyridine derivatives for 48 h. As reported in Table 2, derivatives **14a**, **14b** and **21b** are characterized by a potency on FB789 of the same order of magnitude of the antineoplastic activity in all cancer cell lines evaluated, as expressed by a TSI < 1 (Table 2, entries 1, 2 and 6). Pyrimidine **21a** had a different behavior, showing moderate selectivity on the Huh7 (TSI = 3.3) and Caco-2 (TSI = 5.0) cell lines, but no selectivity on the H9 cell line (Table 2, entries 5). Similarly, compounds **19a,b** displayed high selectivity on the Huh7 (14.0 and 10.2 TSIs for **19a** and **19b**, respectively) and Caco-2 (7.0 and 15.3 TSIs for **19a** and **19b**, respectively) cell lines (Table 2, entries 3 and 4), and low effects on the H9 cell line (0.5 and 1.3 TSIs for **19a** and **19b**, respectively). The difference observed between H9 and Caco-2/Huh7 could be imputable to the different nature and origin of these cell lines, considering that H9 is a suspension cell line derived by lymphoma, while Caco-2 and Huh7 are both adherent epithelial cell lines derived by carcinoma.

Regarding pyridines, derivatives **27a,b** showed a low selectivity (TSI < 3) on H9, Huh7 and Caco-2 cells (Table 2, entries 7 and 8). Compounds **33a** and **38a** are characterized by a low potency on FB789 (Table 2, entries 9 and 11). Pyridines **33b** and **38b** instead

showed high TSI values in all cells evaluated, due to a very low cytotoxic effect on healthy fibroblasts (Table 2, entries 10 and 12), associated with a potency that ranged from 23 μM in the worst case to 8 μM in the best case.

Comparing novel derivatives with original compounds 1–9, it appears that shifting from a triazine core to a pyrimidine and pyridine nuclei led to an increase in TSI values (Tables 1 and 2). In particular, comparison of structurally similar derivatives **19a** and **7** highlights an important increase in TSI on Huh7 in the former (14.0 for **19a** and 3.5 for **7**) and a comparable value in Caco-2 (7.0 vs. 8.8). Pyrimidine **19b** and pyridine **33b** show a robust increase in the TSI with respect to the original triazine **9** in all the three cancer cell lines, as TSIs of the latter never exceeded 0.5. Compound **21a** has a better TSI of 4 in Huh7 (2.8-fold of difference) and in Caco-2 (1.4-fold). Pyridine **33b** is characterized by 50-, 4.8- and 2.5-fold higher TSIs than triazine **6** on H9, Huh7 and Caco-2 cell lines, respectively.

Based on the results obtained using cellular evaluations, further studies aimed at investigating the *in vitro* ADME properties were conducted either on compounds that showed the highest TSI values, such as **19a**, **19b** and **21a**, or the lowest cytotoxic effect on normal cells, products **33b** and **38b** (Figure 2).

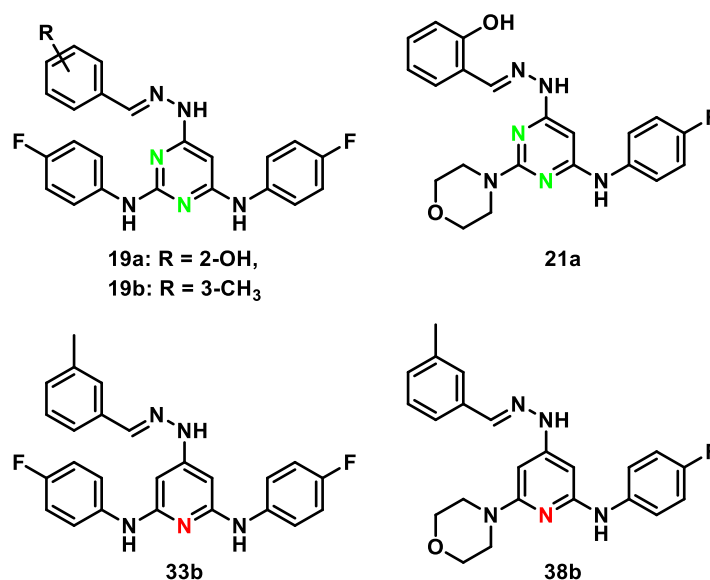


Figure 2. Structure of compounds **19a**, **19b**, **21a**, **33b**, **38b**.

Firstly, the kinetic aqueous solubility of all five derivatives was studied, through the dilution of a DMSO stock solution of these compounds with Mill-Q H₂O followed by incubation for 3 h at room temperature (RT). As reported in Table 3, all pyrimidine derivatives **19a**, **19b**, and **21a** showed suboptimal values of water solubility, less than 0.1 $\mu\text{g}/\text{mL}$ (limit of detection, LOD).

Table 3. Kinetic water solubility of tested compounds.

CPD	$\mu\text{g}/\text{mL}$	LogS ¹	Predicted LogS ²
19a	<0.1	-	-7.50
19b	<0.1	-	-7.82
21a	<0.1	-	-6.69
33b	<0.1	-	-7.87
38b	0.54	-5.87	-5.92

¹ Log of Solubility reported as mol/L. ² LogS data predicted with SwissADME.

Indeed, the presence of the morpholine and phenol moieties in **21a** did not offer a significant improvement to the water solubility in comparison to **19a** (with a phenol group and two para fluorophenyl motifs) or **19b** (with two para fluorophenyl groups and

3-methylphenyl residue). The replacement of the pyrimidine scaffold with a pyridine one slightly enhances the solubility only when one fluorophenyl group was substituted with a morpholine. In fact, if **38b** showed a LogS value of -5.87 , **33b** confirmed the trend seen for **19a**, **19b**, and **21a**. The aqueous solubility of selected compounds was also predicted using the online tool SwissADME; moving from the data obtained for **38b**, the predicted value result was quite similar to the experimental one, suggesting the reliability of the prediction. The predicted values obtained for **19a**, **19b**, **21a**, and **33b** confirmed the suboptimal water solubility of tested derivatives with LogS values between -6.69 and -7.87 .

The parallel artificial membrane permeability assay (PAMPA) underlined a general tendency to efficiently cross membranes. As reported in Table 4, the pyrimidine derivatives **19a**, **19b**, and **21a** showed good apparent permeability values, probably due to the scaffold that reduces the aqueous solubility and promotes the interaction with the phospholipid bilayer. Indeed, **19a** and **19b**, both characterized by two para fluorophenyl groups, resulted in good apparent permeability values and higher percentages of membrane retention (20.99% and 27.42%, respectively) than **21a** endowed with a good passive permeability and a very low membrane retention due to the presence of a morpholine moiety (P_{app} 4.80×10^{-6} cm/s, MR 25.9%).

Table 4. In vitro PAMPA permeability studies of tested compounds.

CPD	P_{app} ¹	MR ² (%)
19a	3.59 ± 0.21	20.91 ± 1.75
19b	5.64 ± 0.59	27.42 ± 1.22
21a	4.80 ± 0.73	26.03 ± 6.17
33b	1.38 ± 0.60	46.84 ± 4.99
38b	6.35 ± 0.67	20.99 ± 1.69

¹ Apparent Permeability (P_{app}) reported in cm/s $\times 10^{-6}$. ² Membrane retention %.

Among the pyridine derivatives, the two para fluorophenyl moieties of **33b** significantly increased the membrane retention up to 46.84% when compared to **38b**, whose percentage remained around 20.99%. In terms of apparent permeability, the high interaction of **33b** with the lipidic bilayer influenced its ability to cross the membrane; indeed, the P_{app} value was noticeably reduced to 1.38×10^{-6} cm/s in comparison to **38b** whose P_{app} value was 6.35×10^{-6} cm/s.

Regarding the stability of tested compounds in the presence of human liver microsomes, the five derivatives showed percentages of metabolic stability never lower than 97%, suggesting a generally high resistance to the transformations induced by liver microsomes (Table 5). Compounds **19a**, **19b**, and **21a** showed very stable results (>99.9%), while **33b** and **38b** underwent a slight metabolization leading to the formation of oxidized derivative M_1 (1.68% and 2.06%, respectively).

Table 5. In vitro metabolic stability studies of tested compounds in the presence of liver microsomes and plasma.

CPD	Metabolic Stability (%)	Metabolite Formation (%) ¹	Plasmatic Stability (%) ²
19a	>99.9	-	86.64 ± 0.17
19b	98.31 ± 0.11	$M_1 = 1.68 \pm 0.11$	>99.9
21a	>99.9	-	96.93 ± 2.73
33b	>99.9	-	81.01 ± 3.28
38b	97.93 ± 0.46	$M_1 = 2.06 \pm 0.46$	87.13 ± 0.48

¹ $M_1 = M + OH (+16)$. ² Plasma stabilities after 24 h of incubation were calculated as percentages of Time 0 taken as 100%.

Finally, the stability in human plasma was investigated by incubating a DMSO solution of compounds in the presence of HEPES buffer and human plasma for 24 h. According to

Table 5, all tested derivatives underwent a slight metabolism, leading to percentages of plasmatic stabilities never lower than 81% after 24 h of incubation.

3. Materials and Methods

3.1. Chemistry—General Part

All reactions were performed in flame-dried glassware under a nitrogen atmosphere. Reagents were obtained from commercial suppliers (Merck Srl, Milan, Italy) and used without further purification. TLC chromatography was performed on precoated aluminum silica gel SIL G/UV254 plates (Macherey-Nagel & Co., Düren, Deutschland). The detection occurred via fluorescence quenching or development in a ninhydrin solution (0.2 g of ninhydrin in 99.5 mL ethanol and 0.5 mL acetic acid.). Merck silica gel 60 was used for flash chromatography (23–400 mesh). ^1H NMR and ^{13}C NMR spectra were measured on a Bruker (Billerica, MA, USA) Avance DRX400 (400 MHz/100 MHz) spectrometer. Chemical shifts for protons are reported in parts per million (ppm, δ scale) and internally referenced to the deuterated dimethyl sulfoxide (DMSO- d_6), methanol (CD $_3$ OD) or chloroform (CDCl $_3$) signal at δ 2.50, 3.33 and 7.28 ppm, respectively. ^1H -NMR spectra are reported first by their multiplicity and then by their number of protons; signals are characterized as: s (singlet), d (doublet), dd (doublet of doublets), ddd (doublet of doublet of doublets), t (triplet), m (multiplet), bs (broad signal). 2,4,6-trichlorotriazine, 2,4,6-trichloropyrimidine and 2,4,6-trifluoropyridine were bought from Merck Srl (Milan, Italy).

Microwave irradiation experiments were conducted using a CEM Discover Synthesis Unit (CEM Corp., Matthews, NC, USA). The apparatus consists of a continuous focused microwave power delivery system with an operator-selectable power output of 0 to 300 W. The temperature of the contents of the tube was monitored using a calibrated IR temperature control mounted under the reaction tube. All experiments were performed using a stirring option where the contents of the tube are stirred by means of a rotating magnetic plate located below the floor of the microwave cavity and a Teflon-coated magnetic stir bar in the tube.

Mass detection of compounds was performed using an Agilent 1260 Infinity HPLC-DAD system connected to an Agilent MSD 6130 system (Agilent Technologies, Palo Alto, CA, USA) as described in the UV/LC-MS method section below. High-Resolution Mass Spectra (HRMS) were recorded on an LC-MS/MS system (Q Executive Plus; Thermo Scientific, Waltham, MA, USA).

3.2. Chemistry—Experimental Procedures and Compound Characterization

The procedure for the synthesis of monosubstituted pyrimidine derivatives **11** and **12** is as follows:

To a solution of 2,4,6-trichloropyrimidine **10** (1 equiv.) in CH $_2$ Cl $_2$ (10 mL) at 0 °C, morpholine (1 equiv.) was slowly added, followed by DIPEA (1 equiv.). The reaction mixture was stirred at 0 °C for 5 h, and then warmed up to 25 °C. The mixture was washed with H $_2$ O and brine. The organic phase was dried over anhydrous Na $_2$ SO $_4$ and evaporated to dryness. The resulting residue was purified through column chromatography using a mixture of petroleum ether (PET)/ethyl acetate (EtOAc) 4:1 to give the desired products **11** and **12** with 19% and 68% yield, respectively.

Compound **11**

R_f = 0.29 (PET/EtOAc 4:1); ^1H NMR (400 MHz, CDCl $_3$) δ 6.57 (s, 1H), 3.83 (d, J = 5.2 Hz, 4H), 3.76 (d, J = 4.8 Hz, 4H) ppm. ^{13}C NMR (100 MHz, CDCl $_3$) δ 161.8, 160.6, 108.3, 66.6, 44.4 ppm. MS m/z for C $_8$ H $_{10}$ Cl $_2$ N $_3$ O, (ESI $^+$) m/z : 234.0 [M + H] $^+$.

Compound **12**

R_f = 0.26 (PET/EtOAc 4:1); ^1H NMR (400 MHz, CDCl $_3$) δ 6.41 (s, 1H), 3.79–3.77 (m, 4H), 3.65 (s, 4H) ppm. ^{13}C NMR (100 MHz, CDCl $_3$) δ 163.3, 160.7, 159.9, 99.7, 66.2, 44.6 ppm. MS m/z for C $_8$ H $_{10}$ Cl $_2$ N $_3$ O, (ESI $^+$) m/z : 234.0 [M + H] $^+$.

*Procedure for the synthesis of disubstituted pyrimidine derivative **13***

Compound **12** (1 equiv.) was dissolved in 1,4-dioxane (10 mL) and morpholine (2.5 equiv.) was added. Then, a few drops of HCl were slowly added. The reaction was conducted under microwave irradiation for 40 min at 110 °C. After cooling to 25 °C, the mixture was washed with H₂O and brine. The organic phase was dried over anhydrous Na₂SO₄ and evaporated to dryness. The solid residue obtained was purified using column chromatography using diethyl ether (Et₂O)/PET 2:1 as eluant to give the disubstituted intermediate **13** with 90% yield.

R_f = 0.26 (Et₂O/PET); ¹H NMR (400 MHz, CDCl₃) δ 5.87 (s, 1H), 3.76–3.73 (m, 8H), 3.56–3.54 (m, 8H) ppm. ¹³C NMR (100 MHz, CDCl₃) δ 163.5, 160.8, 160.6, 91.1, 66.8, 66.5, 44.4, 44.3 ppm. MS *m/z* for C₁₂H₁₈ClN₄O₂, (ESI⁺) *m/z*: 285.1 [M + H]⁺.

General Procedure for the synthesis of trisubstituted pyrimidine derivatives 14a,b

Compound **13** (1 equiv.) was dissolved in 1,4-dioxane (1 mL) and hydrazine hydrate (20 equiv.) was added. The reaction was stirred under microwave irradiation for 4 h at 100 °C. After this time, the reaction mixture was diluted with EtOAc and then was washed with H₂O and brine, dried over anhydrous Na₂SO₄ and evaporated to dryness. The crude residue was pure enough to be subjected to the next step.

To a solution of hydrazine derivative (1 equiv.) in MeOH (10 mL), the opportune aldehyde (1 equiv.) and a drop of acetic acid were added. The mixture was stirred for 24 h at 25 °C. The precipitate formed was filtered-off and dried under high vacuum giving the desired products **14a,b** with 55 and 65% yield, respectively.

Compound 14a

R_f = 0.19 (hexane (Hex)/EtOAc 1:1). ¹H-NMR (400 MHz, CDCl₃) δ 10.70 (bs, 1H), 8.53 (bs, 1H), 7.90 (s, 1H), 7.31–7.26 (m, 1H), 7.19 (d, *J* = 6.8 Hz, 1H), 7.00 (d, *J* = 8.4 Hz, 1H), 6.93 (t, *J* = 7.2 Hz, 1H), 5.56 (s, 1H), 3.80–3.73 (m, 12H), 3.61–3.57 (m, 4H) ppm. ¹³C NMR (100 MHz, CDCl₃) δ 164.1, 160.6, 157.3, 144.0, 130.9, 130.1, 119.7, 118.0, 116.6, 72.9, 66.9, 66.7, 44.6, 44.5 ppm. MS *m/z* for C₁₉H₂₅N₆O₃, (ESI⁺) *m/z*: 385.2 [M + H]⁺. HRMS (ESI) *m/z* for C₁₉H₂₅N₆O₃ = 385.1983 [M + H]⁺, found 385.1985; elemental analysis calcd. (%) for C₁₉H₂₄N₆O₃: C, 59.36; H, 6.29; N, 21.86; O, 12.48; found: C, 59.34; H, 6.29; N, 21.86; O, 12.49.

Compound 14b

R_f = 0.25 (Hex/EtOAc 1:1). ¹H NMR (400 MHz, CDCl₃) δ 8.14 (bs, 1H), 7.69 (bs, 1H), 7.48–7.45 (m, 2H), 7.31–7.25 (m, 1H), 7.17 (d, *J* = 7.2 Hz, 1H), 5.92 (s, 1H), 3.82–3.79 (m, 4H), 3.74–3.72 (m, 8H), 3.64–3.62 (m, 4H), 2.40 (s, 3H). ¹³C NMR (100 MHz, CDCl₃) δ 164.3, 162.5, 161.1, 140.5, 138.3, 134.5, 130.1, 128.6, 127.2, 123.9, 73.8, 67.0, 66.8, 44.7, 44.5, 21.4 ppm. MS *m/z* for C₂₀H₂₇N₆O₂, (ESI⁺) *m/z*: 383.2 [M + H]⁺. HRMS (ESI) *m/z* for C₂₀H₂₇N₆O₂ = 383.2190 [M + H]⁺, found 383.2191; elemental analysis calcd. (%) for C₂₀H₂₆N₆O₂: C, 62.81; H, 6.85; N, 21.97; O, 8.37; found: C, 62.80; H, 6.85; N, 21.97; O, 8.38.

Procedure for the Synthesis of monosubstituted pyrimidine intermediate 16 and 17

To a solution of 2,4,6-trichloropyrimidine **10** (1 equiv.) in CH₂Cl₂ (10 mL) at 0 °C, 4-fluoroaniline (1 equiv.) was slowly added, followed by DIPEA (1 equiv.). The obtained reaction mixture was stirred at 0 °C for 5 h, and then warmed up to 25 °C. The mixture was washed with water, dried over N₂SO₄ and the solvent removed under reduced pressure. The crude residue was purified using column chromatography PET/EtOAc 4:1 to give the desired products **16** and **17** with 14 and 75% yield, respectively.

Compound 16

R_f = 0.29 (PET/EtOAc 4:1). ¹H NMR (400 MHz, CDCl₃) δ 7.53–7.50 (m, 2H), 7.09–7.04 (m, 2H), 6.80 (s, 1H) ppm. ¹³C NMR (100 MHz, CDCl₃) δ 162.0, 159.8 (d, *J* = 149.0 Hz), 158.1, 133.7, 121.9 (d, *J* = 7.9 Hz), 115.8 (d, *J* = 22.5 Hz), 115.7, 111.3 ppm. MS *m/z* for C₁₀H₇Cl₂FN₃, (ESI⁺) *m/z*: 258.0 [M + H]⁺.

Compound 17

R_f = 0.22 (PET/EtOAc 4:1). ¹H NMR (400 MHz, CDCl₃) δ 7.30–7.27 (m, 2H), 7.17–7.13 (m, 2H), 6.44 (s, 1H) ppm. ¹³C NMR (100 MHz, CDCl₃) δ 163.6, 161.8 (d, *J* = 116.0 Hz), 160.2, 160.0, 132.1, 126.4 (d, *J* = 7.1 Hz), 116.9 (d, *J* = 22.7 Hz), 100.7 ppm. MS *m/z* for C₁₀H₇Cl₂FN₃, (ESI⁺) *m/z*: 258.0 [M + H]⁺.

Procedure for the synthesis of disubstituted pyrimidine intermediate 18

Compound **17** was dissolved in 1,4-dioxane (10 mL) and 4-fluoroaniline (2.5 eq) was added. Then, a few drops of HCl were slowly added to the mixture. The reaction was conducted under microwave irradiation for 40 min at 110 °C. The mixture was washed with water, brine and dried over N_2SO_4 . The residue was purified using column chromatography with CH_2Cl_2 as eluant. The purified material was dried in vacuo to afford the desired product with 62% yield.

$R_f = 0.20$ (CH_2Cl_2); 1H NMR (400 MHz, $CDCl_3$) δ 7.49–7.46 (m, 2H), 7.31–7.27 (m, 2H), 7.11–7.06 (m, 2H), 7.03–6.99 (m, 2H), 6.98 (s, 1H), 6.06 (s, 1H) ppm. ^{13}C NMR (100 MHz, $CDCl_3$) δ 162.7, 159.9 (d, $J = 100.1$ Hz), 157.6, 134.8, 133.5, 125.4 (d, $J = 8.0$ Hz), 121.8 (d, $J = 7.7$ Hz), 116.3 (d, $J = 22.6$ Hz), 115.5 (d, $J = 22.3$ Hz), 94.4 ppm. MS m/z for $C_{16}H_{12}ClF_2N_4$, (ESI⁺) m/z : 333.1 [M + H]⁺.

General procedure for the synthesis of trisubstituted pyrimidine derivatives 19a,b

Compound **18** (1 equiv.) was dissolved in 1,4-dioxane (1 mL) and hydrazine hydrate (20 equiv.) was added. The reaction was stirred under microwave irradiation for 4 h at 100 °C. After this time, the reaction mixture was diluted with EtOAc and then washed with H_2O and brine, and dried over N_2SO_4 . The crude residue was pure enough to be subjected to the next step.

To a solution of hydrazine derivative (1 equiv.) in MeOH (10 mL), the opportune aldehyde (1 equiv.) and a drop acetic acid were added. The mixture was stirred for 48 h at 25 °C. The precipitate that formed was filtered-off and dried under a high vacuum giving the desired products **19a,b** with 53 and 61% yield, respectively.

Compound 19a

$R_f = 0.42$ (Hex/EtOAc 1:1) 1H -NMR (400 MHz, CD_3OD) δ 8.11 (s, 1H), 7.67 (dd, $J = 8.8$ Hz $J = 4.4$ Hz, 2H), 7.55 (dd, $J = 8.8$ Hz $J = 4.8$ Hz, 2H), 7.29 (d, $J = 6.4$ Hz, 1H), 7.25 (d, 1H), 7.04–7.00 (m, 4H), 6.98–6.90 (m, 2H), 5.76 (s, 1H) ppm. ^{13}C NMR (100 MHz, CD_3OD) δ 162.4, 160.5 (d, $J = 145.2$ Hz), 159.1, 157.1, 156.7, 143.5, 137.0, 136.6, 130.0, 129.4, 122.4 (d, $J = 7.6$ Hz), 120.9 (d, $J = 7.4$ Hz), 119.2, 118.8, 115.9, 114.7 (d, $J = 22.3$ Hz), 114.3 (d, $J = 22.2$ Hz), 76.1 ppm. MS m/z for $C_{23}H_{19}F_2N_6O$, (ESI⁺) m/z : 433.2 [M + H]⁺. HRMS (ESI) m/z for $C_{23}H_{19}F_2N_6O = 433.1583$ [M + H]⁺, found 433.1585; elemental analysis calcd. (%) for $C_{23}H_{18}F_2N_6O$: C, 63.88; H, 4.20; F, 8.79; N, 19.43; O, 3.70; found: C, 63.87; H, 4.20; F, 8.79; N, 19.43; O, 3.72.

Compound 19b

$R_f = 0.30$ (Hex/EtOAc 1:1). 1H NMR (400 MHz, CD_3OD) δ 7.88 (s, 1H), 7.67–7.64 (m, 2H), 7.57–7.54 (m, 2H), 7.51 (s, 1H), 7.43 (d, $J = 7.6$ Hz, 1H), 7.26 (t, $J = 7.6$ Hz, 1H), 7.15 (d, $J = 7.6$, 2H), 7.04–6.95 (m, 4H), 6.09 (s, 1H), 2.36 (s, 3H) ppm. ^{13}C NMR (100 MHz, CD_3OD) δ 162.3, 160.9 (d, $J = 257.2$ Hz), 159.1, 157.2, 156.7, 140.9, 138.0, 135.3, 129.4, 128.1, 126.5, 123.5, 122.3 (d, $J = 7.5$ Hz), 121.0 (d, $J = 7.4$ Hz), 114.6 (d, $J = 22.3$ Hz), 114.3 (d, $J = 22.2$ Hz), 76.9, 20.0 ppm. MS m/z for $C_{24}H_{21}F_2N_6$, (ESI⁺) m/z : 431.2 [M + H]⁺. HRMS (ESI) m/z for $C_{24}H_{21}F_2N_6 = 431.1790$ [M + H]⁺, found 431.1792; elemental analysis calcd. (%) for $C_{24}H_{20}F_2N_6$: C, 66.97; H, 4.68; F, 8.83; N, 19.52; found: C, 66.95; H, 4.69; F, 8.83; N, 19.53.

Procedure for the synthesis of disubstituted pyrimidine 20

To a solution of compound **17** (1 equiv.) in EtOH (10 mL), morpholine (1 equiv.) and triethyl amine (1.5 equiv.) were added. The reaction mixture was stirred at 80 °C for 18 h. After this time, the solvent was evaporated under reduced pressure and the residue was washed with water and brine, and dried over Na_2SO_4 . The obtained crude was purified using column chromatography using $CH_2Cl_2/MeOH$ (10 mL:100 μ L) as eluant. The purified material was dried in vacuo to afford the desired product with 62% yield.

$R_f = 0.20$ ($CH_2Cl_2/MeOH$ 10mL:100 μ L). 1H NMR (400 MHz, $CDCl_3$) δ 7.29–7.26 (m, 2H), 7.08–7.04 (m, 2H), 6.55 (s, 1H), 5.89 (s, 1H), 3.75 (d, $J = 4$ Hz, 8H) ppm. ^{13}C NMR (100 MHz, $CDCl_3$) δ 164.3, 161.6 (d, $J = 200.2$ Hz), 158.0, 135.5, 124.2 (d, $J = 7.1$ Hz), 115.9 (d, $J = 22.4$ Hz), 73.9, 67.0, 66.6, 44.6, 44.5 ppm. MS m/z for $C_{14}H_{15}ClFN_4O$, (ESI⁺) m/z : 309.1 [M + H]⁺.

Procedure for the synthesis of disubstituted pyrimidine 21a,b

Compound **20** (1 equiv.) was dissolved in 1,4-dioxane (1 mL) and hydrazine hydrate (20 equiv.) was added. The reaction was stirred under microwave irradiation for 6 h at 100 °C. After this time, the reaction mixture was diluted with EtOAc and then washed with H₂O and brine, and dried over N₂SO₄. The crude residue was pure enough to be subjected to the next step.

To a solution of hydrazine derivative (1 equiv.) in MeOH (10 mL), the opportune aldehyde (1 equiv.) and a drop acetic acid were added. The mixture was stirred for 48 h at 25 °C. The precipitate formed was filtered-off and dried under high vacuum giving the desired products **21a,b** with 46% and 45% yield, respectively.

Compound **21a**

R_f = 0.18 (CH₂Cl₂/MeOH 10:0,2). ¹H-NMR (400 MHz, CDCl₃) δ 10.48 (bs, 1H), 8.08 (bs, 1H), 7.88 (s, 1H), 7.36–7.33 (m, 2 H), 7.29–7.26 (m, 1H), 7.18 (dd, *J* = 7.6 Hz, *J* = 1.6 Hz, 1H), 7.08 (t, *J* = 8.8 Hz, 2 H), 7.00 (d, *J* = 7.6 Hz, 1H), 6.92 (t, *J* = 8.4 Hz, 1H), 6.45 (bs, 1H), 5.67 (s, 1H), 3.76 (s, 8H) ppm. ¹³C-NMR (100 MHz, CDCl₃) δ 162.3, 161.0, 159.3 (d, *J* = 251.4 Hz), 157.4, 144.2, 135.0, 131.0, 130.1, 123.6 (d, *J* = 8.0 Hz), 119.6, 117.9, 116.8, 115.9 (d, *J* = 22.4 Hz), 74.6, 66.9, 44.6 ppm. MS *m/z* for C₂₁H₂₂FN₆O₂, (ESI⁺) *m/z*: 409.2 [M + H]⁺. HRMS (ESI) *m/z* for C₂₁H₂₂FN₆O₂ = 409.1783 [M+H]⁺, found 409.1781; elemental analysis calcd. (%) for C₂₁H₂₁FN₆O₂: C, 61.76; H, 5.18; F, 4.65; N, 20.58; O, 7.83; found: C, 61.75; H, 5.19; F, 4.65; N, 20.58; O, 7.84.

Compound **21b**

R_f: 0.29 (CH₂Cl₂/MeOH 10:0,2) ¹H NMR (400 MHz, CDCl₃) δ 8.10 (bs, 1H), 7.69 (s, 1H), 7.44 (s, 1H), 7.41–7.35 (m, 3H), 7.29–7.25 (m, 1H), 7.18 (d, *J* = 7.6 Hz, 1H), 7.09–7.04 (m, 2H), 6.39 (bs, 1H), 6.03 (s, 1H), 3.76 (s, 8H), 2.38 (3H) ppm. ¹³C NMR (100 MHz, DMSO-*d*₆) δ 162.4, 161.8, 160.0 (d, *J* = 309.8 Hz), 156.1, 140.8, 138.4, 138.0, 135.6, 130.0, 129.1, 126.8, 123.9, 121.1 (d, *J* = 7.4 Hz), 115.5 (d, *J* = 21.8 Hz), 76.5, 66.6, 44.7, 21.5 ppm. MS *m/z* for C₂₂H₂₄FN₆O, (ESI⁺) *m/z*: 407.2 [M + H]⁺. HRMS (ESI) *m/z* for C₂₂H₂₄FN₆O = 407.1990 [M + H]⁺, found 407.1991; elemental analysis calcd. (%) for C₂₂H₂₃FN₆O: C, 65.01; H, 5.70; F, 4.67; N, 20.68; O, 3.94; found: C, 65.00; H, 5.71; F, 4.67; N, 20.68; O, 3.95.

Procedure for the synthesis of monosubstituted pyridine derivatives **23** and **24**

To a solution of morpholine (1 equiv.) and Et₃N (2.5 equiv.) in dry THF (5 mL), a solution of 2,4,6-trichloropyridine **22** (1 equiv.) in THF (2 mL) was added. The reaction mixture was stirred 24 h at 65 °C. After cooling to 25 °C, the reaction was concentrated to remove THF and then diluted with Et₂O and washed with water and brine, dried over anhydrous Na₂SO₄, and filtered and evaporated in vacuo. The crude mixture was purified via column chromatography using Hex/EtOAc 5:1 as the eluant to give **23** and **24** with 15 and 30% yield, respectively.

Compound **23**

R_f = 0.17 (Hex/EtOAc 5:1). ¹H NMR (400 MHz, CDCl₃) δ 6.57 (s, 2H), 3.81 (t, *J* = 4 Hz, 4H), 3.30 (t, *J* = 4 Hz, 4H) ppm. ¹³C NMR (100 MHz, CDCl₃) δ 158.0, 151.2, 106.2, 66.0, 46.1 ppm. MS *m/z* for C₉H₁₁Cl₂N₂O, (ESI⁺) *m/z*: 233.0 [M + H]⁺.

Compound **24**

R_f = 0.40 (Hex/EtOAc 5:1). ¹H NMR (400 MHz, CDCl₃) δ = 6.66 (d, *J* = 1.2 Hz, 1H), 6.47 (d, *J* = 4 Hz, 1H), 3.79 (t, *J* = 4.8 Hz, 4H), 3.53 (t, *J* = 4 Hz, 4H) ppm. ¹³C NMR (100 MHz, CDCl₃) δ 159.2, 150.2, 146.3, 112.6, 104.4, 66.4, 45.1 ppm. MS *m/z* for C₉H₁₁Cl₂N₂O, (ESI⁺) *m/z*: 233.0 [M + H]⁺.

Procedure for the Synthesis of disubstituted pyridine derivatives **25** and **28**

To a solution of monosubstituted pyridine **24** (1 equiv.) in DMF (2 mL), morpholine (10 equiv.) and DIPEA (3 equiv.) was added. The mixture was warmed at 120 °C for 48 h. After cooling to 25 °C, the reaction mixture was diluted with CH₂Cl₂ and washed with an aqueous solution of 3% LiCl. The organic phase was dried over anhydrous Na₂SO₄, and filtered and evaporated in vacuo to afford a crude mixture of two regioisomers. Products **25** and **28** can be separated through column chromatography using a mixture of Hex/EtOAc 2:1, and recovered with 58 and 18% yield, respectively.

Compound **25**

$R_f = 0.45$ (Hex/EtOAc 2:1)] $^1\text{H NMR}$ (400 MHz, CDCl_3) δ 6.0 (s, 2H), 3.79 (d, $J = 4$ Hz, 8H), 3.47 (d, $J = 8$ Hz, 8H) ppm. $^{13}\text{C NMR}$ (100 MHz, CDCl_3) δ 158.2, 146.8, 97.0, 66.7, 49.3 ppm. MS m/z for $\text{C}_{13}\text{H}_{19}\text{ClN}_3\text{O}_2$, (ESI $^+$) m/z : 284.1 $[\text{M} + \text{H}]^+$.

Compound 28

$R_f = 0.13$ (Hex/EtOAc 2:1). $^1\text{H NMR}$ (400 MHz, CDCl_3) δ 6.20 (d, $J = 4$ Hz, 1H), 5.77 (d, $J = 1,2$ Hz, 1H), 3.82–3.78 (m, 8H), 3.46 (t, $J = 4$ Hz, 4H), 3.25 (t, $J = 4$ Hz, 4H) ppm. $^{13}\text{C NMR}$ (100 MHz, CDCl_3) δ 159.2, 150.2, 146.3, 112.6, 104.4, 66.4, 45.1 ppm. MS m/z for $\text{C}_{13}\text{H}_{19}\text{ClN}_3\text{O}_2$, (ESI $^+$) m/z : 284.1 $[\text{M} + \text{H}]^+$.

Procedure for the synthesis of Boc-protected trisubstituted pyridine carbazate 26

In a microwave tube, compound **25** (1 equiv.), *tert*-butyl carbazate (BocNHNH_2 , 10 equiv.), $\text{Pd}_2(\text{dba})_3$ (0.04 equiv.), DPPF (0.12 equiv.), Cs_2CO_3 (2 equiv.) and dry toluene (1 mL) were added under an argon atmosphere. The reaction mixture was stirred at 150 °C for 10 min under microwave irradiation. The mixture was filtered through celite, rinsed with EtOAc and concentrated. The crude was purified using column chromatography with $\text{CH}_2\text{Cl}_2/\text{EtOAc}$ 4:1 as the eluant to produce the product **26** with 65% yield.

$R_f = 0.43$ (Hex/EtOAc 2:1)] $^1\text{H NMR}$ (400 MHz, CDCl_3) δ 6.2 (s, 2H), 3.98–3.85 (m, 8H), 3.81 (t, $J = 4.8$ Hz, 4H), 3.50 (t, $J = 4.4$ Hz, 4H), 1.49 (s, 3H) ppm. $^{13}\text{C NMR}$ (100 MHz, CDCl_3) δ 159.0, 154.4, 153.2, 89.9, 82.6, 66.9, 46.0, 28.3 ppm. MS m/z for $\text{C}_{18}\text{H}_{30}\text{N}_5\text{O}_4$, (ESI $^+$) m/z : 380.2 $[\text{M} + \text{H}]^+$.

Procedure for the synthesis of trisubstituted pyridine derivatives 27a,b

Boc-protected pyridine **26** (1 equiv.) was dissolved in anhydrous CH_2Cl_2 (430 μL) and cooled to 0 °C. TFA (290 μL) was added, and the reaction mixture was warmed to 25 °C and stirred for 1 h. After this time, the mixture was concentrated at reduced pressure. The residue obtained was pure enough to be subjected to the next step.

To a solution of hydrazine derivative (1 equiv.) in MeOH (10 mL), the opportune aldehyde (1 equiv.) and few drops of acetic acid were added. The mixture was stirred for 24 h at 25 °C and concentrated under vacuum. The residue was purified using column chromatography (Hex/EtOAc 2:1), furnishing the desired products **27a,b** with 39% and 18% yield, respectively.

Compound 27a

$R_f = 0.40$ (Hex/EtOAc 1:1). $^1\text{H NMR}$ (400 MHz, CDCl_3) δ 10.93 (s, 1H), 8.39 (s, 1H), 7.86 (s, 1H), 7.27–7.24 (m, 1H), 7.15 (dd, $J = 7.6$ Hz, $J = 1.6$ Hz, 1H), 6.99 (d, $J = 8.0$ Hz, 1H), 6.92–6.90 (m, 1H), 5.96 (m, 1H), 3.85–3.78 (m, 8H), 3.44 (t, $J = 4.0$ Hz, 4H), 3.31 (t, $J = 4.0$ Hz, 4H) ppm. $^{13}\text{C NMR}$ (CDCl_3 , 100 Hz) δ 160.2, 159.6, 157.1, 155.3, 141.7, 130.2, 129.5, 119.6, 118.5, 116.5, 82.1, 66.8, 66.6, 47.0, 46.2 ppm. MS m/z for $\text{C}_{20}\text{H}_{26}\text{N}_5\text{O}_3$, (ESI $^+$) m/z : 384.2 $[\text{M} + \text{H}]^+$. HRMS (ESI) m/z for $\text{C}_{20}\text{H}_{26}\text{N}_5\text{O}_3 = 384.2030$ $[\text{M} + \text{H}]^+$, found 384.2031; elemental analysis calcd. (%) for $\text{C}_{20}\text{H}_{25}\text{N}_5\text{O}_3$: C, 62.65; H, 6.57; N, 18.26; O, 12.52; found: C, 62.64; H, 6.58; N, 18.26; O, 12.53.

Compound 27b

$R_f = 0.55$ (Hex/EtOAc 2:1). $^1\text{H NMR}$ (400 MHz, CDCl_3) δ 8.11 (s, 1H), 7.66 (s, 1H), 7.47 (d, $J = 8.0$ Hz, 2H), 7.27 (t, $J = 8.0$ Hz, 1H), 7.14 (d, $J = 8.0$ Hz, 1H), 6.33–6.32 (m, 1H), 3.86–3.80 (m, 8H), 3.42 (t, $J = 8.0$ Hz, 4H), 3.33 (t, $J = 8.0$ Hz, 4H), 2.39 (s, 3H) ppm. $^{13}\text{C NMR}$ (CDCl_3 , 100 Hz) δ 163.3, 159.4, 153.8, 141.8, 146.2, 138.3, 134.2, 130.7, 128.5, 127.9, 124.1, 81.2, 66.2, 66.1, 46.3, 21.4 ppm. MS m/z for $\text{C}_{21}\text{H}_{28}\text{N}_5\text{O}_2$, (ESI $^+$) m/z : 382.2 $[\text{M} + \text{H}]^+$. HRMS (ESI) m/z for $\text{C}_{21}\text{H}_{28}\text{N}_5\text{O}_2 = 382.2238$ $[\text{M} + \text{H}]^+$, found 382.2239; elemental analysis calcd. (%) for $\text{C}_{21}\text{H}_{27}\text{N}_5\text{O}_2$: C, 66.12; H, 7.13; N, 18.36; O, 8.39; found: C, 66.13; H, 7.14; N, 18.36; O, 8.37.

Procedure for the synthesis of monosubstituted pyridine derivatives 29 and 30

In a two necks flask equipped with molecular sieves, 2,4,6-trichloropyridine **22** (1 equiv.), Cs_2CO_3 (1 equiv.), $\text{Pd}(\text{PPh}_3)_4$ (0.02 equiv.) and dry toluene (5 mL) were added. Subsequently, 4-fluoroaniline (1.6 equiv.) was added under an argon atmosphere and the reaction mixture was stirred for 24 h at 150 °C. After this time, the mixture was filtered through celite, rinsed with EtOAc and concentrated. The residue obtained was diluted with EtOAc, washed with a saturated aqueous solution of NaHCO_3 and brine, dried over Na_2SO_4 and concentrated under reduced pressure. The crude was purified using column

chromatography with Pet/EtOAc 4:1 as eluant to give the products **29** and **30** with 19 and 50% yield, respectively.

Compound 29

$R_f = 0.50$ (Pet/EtOAc 4:1). $^1\text{H NMR}$ (400 MHz, CDCl_3) δ 7.27 (m, 2H), 7.12 (t, $J = 8.4$ Hz, 2H), 7.00 (s, 1H), 6.7 (s, 2H) ppm. ^{13}C (100 MHz, CDCl_3) δ 159.3 (d, $J = 241.9$ Hz), 156.2, 146.3, 135.6, 123.8 (d, $J = 6.9$ Hz), 116.0 (d, $J = 22.3$ Hz), 98.0 ppm. MS m/z for $\text{C}_{11}\text{H}_8\text{Cl}_2\text{FN}_2$, (ESI⁺) m/z : 257.0 [M + H]⁺.

Compound 30

$R_f = 0.65$ (Pet/EtOAc 4:1). $^1\text{H NMR}$ (400 MHz, CDCl_3) δ 7.26 (m, 2H), 7.09 (t, $J = 8.8$ Hz, 2H), 7.00 (s, 1H), 6.73 (d, $J = 1.2$ Hz, 1H), 6.54 (d, $J = 1.2$ Hz, 1H) ppm. ^{13}C NMR (100 MHz, CDCl_3) δ 160.0 (d, $J = 240.3$ Hz), 157.2, 150.5, 146.6, 134.5, 124.8 (d, $J = 8.1$ Hz), 116.4 (d, $J = 22.6$ Hz), 114.2, 104.9 ppm. MS m/z for $\text{C}_{11}\text{H}_8\text{Cl}_2\text{FN}_2$, (ESI⁺) m/z : 257.0 [M + H]⁺.

Procedure for the synthesis of disubstituted pyridine derivatives 31 and 34

$\text{Pd}(\text{OAc})_2$ (0.02 equiv.) and BINAP (0.02 equiv.) were dissolved in anhydrous toluene (1 mL) and the mixture was kept under argon for 10 min. At the same time, compound **30** (1 equiv.), anhydrous toluene (1 mL), Cs_2CO_3 (3.5 equiv.), and 4-fluoroaniline (1.5 equiv.) and then the solution of $\text{Pd}(\text{OAc})_2$ and BINAP above described were put into a Schenck tube. The reaction mixture was warmed at 160 °C and left under stirring for 4 h. After this time, the mixture was filtered through celite, rinsed with EtOAc and concentrated. The crude was purified using column chromatography with Pet/EtOAc 3:1 as eluant to give the products **31** and **34** with 36 and 13% yield, respectively.

Compound 31

$R_f = 0.63$ (Pet/EtOAc 3:1). $^1\text{H NMR}$ (400 MHz, CDCl_3) δ 7.29 (m, 4H), 7.06 (m, 4H), 6.65 (s, 1H), 6.13 (s, 2H) ppm. ^{13}C NMR (100 MHz, CDCl_3) δ 159.2 (d, $J = 260.2$ Hz), 156.0, 146.6, 135.4, 123.9 (d, $J = 7.9$ Hz), 116.1 (d, $J = 22.4$ Hz), 98.0 ppm. MS m/z for $\text{C}_{17}\text{H}_{13}\text{ClF}_2\text{N}_3$, (ESI⁺) m/z : 332.1 [M + H]⁺.

Compound 34

$R_f = 0.44$ (Pet/EtOAc 3:1). $^1\text{H NMR}$ (400 MHz, CDCl_3) δ 7.21 (m, 4H), 7.11 (m, 4H), 6.45 (s, 1H), 6.24 (d, $J = 1.6$ Hz, 1H), 6.0 (d, $J = 1.6$ Hz, 1H), 5.9 (s, 1H) ppm. ^{13}C (100 MHz, CDCl_3) δ 159.2 (d, $J = 270.4$ Hz), 156.8, 148.1, 141.5, 136.5, 123.4 (d, $J = 7.4$ Hz), 116.3 (d, $J = 22.4$ Hz), 100.0, 94.0 ppm. MS m/z for $\text{C}_{17}\text{H}_{13}\text{ClF}_2\text{N}_3$, (ESI⁺) m/z : 332.1 [M + H]⁺.

Procedure for the synthesis of Boc-protected trisubstituted pyridine carbazate 32

In a microwave tube, compound **31** (1 equiv.), BocNHNH_2 (10 equiv.), $\text{Pd}_2(\text{dba})_3$ (0.04 equiv.), DPPF (0.12 equiv.), Cs_2CO_3 (2 equiv.) and dry toluene (1 mL) were added under an argon atmosphere. The reaction mixture was stirred at 150 °C for 10 min under microwave irradiation. The mixture was filtered through celite, rinsed with EtOAc and concentrated. The crude was purified using column chromatography with Hex/EtOAc 2:1 as eluant to produce the product **32** with 59% yield.

$R_f = 0.37$ (Hex/EtOAc 2:1). $^1\text{H NMR}$ (400 MHz, CDCl_3): δ 7.31 (m, 4H), 7.03 (m, 4H), 6.61 (s, 2H), 5.32 (s, 1H), 4.24 (s, 1H), 1.49 (s, 3H) ppm. ^{13}C NMR (100 MHz, CDCl_3) δ 158.8 (d, $J = 240.2$ Hz), 155.6, 154.2, 153.3, 136.5, 123.0 (d, $J = 7.7$ Hz), 115. (d, $J = 22.2$ Hz), 90.9, 83.1, 28.2 ppm. MS m/z for $\text{C}_{22}\text{H}_{24}\text{F}_2\text{N}_5\text{O}_2$, (ESI⁺) m/z : 428.2 [M + H]⁺.

Procedure for the synthesis of trisubstituted pyridine derivatives 33a,b

Boc-protected pyridine **32** (1 equiv.) was dissolved in anhydrous CH_2Cl_2 (430 μL) and cooled to 0 °C. TFA (290 μL) was added, and the reaction mixture was warmed to 25 °C and stirred for 1 h. After this time, the mixture was concentrated at reduced pressure. The residue obtained was pure enough to be subjected to the next step.

To a solution of hydrazine derivative (1 equiv.) in MeOH (10 mL), the opportune aldehyde (1 equiv.) and few drops of acetic acid were added. The mixture was stirred for 24 h at 25 °C and concentrated under vacuum. The residue was purified using column chromatography (Hex/EtOAc 1:1) furnishing the desired products **33a,b** with 29% and 21% yield, respectively.

Compound 33a

$R_f = 0.37$ (Hex/EtOAc 1:1). ^1H NMR (400 MHz, CDCl_3) δ 10.47 (bs, 1H), 7.81 (s, 1H), 7.57 (bs, 1H), 7.33–7.27 (m, 5H), 7.15 (d, $J = 7.6$ Hz, 2H), 7.07–6.98 (m, 5H), 6.92 (t, $J = 7.6$ Hz, 1H), 6.36 (bs, 2H), 5.81 (s, 2H) ppm. ^{13}C (100 MHz, CD_3OD) δ 161.6, 159.4 (d, $J = 69.8$ Hz), 159.3, 157.4, 156.0, 140.7, 139.4, 136.9, 136.6, 131.0, 126.7, 122.5 (d, $J = 10.9$ Hz), 121.2, 119.6, 114.7 (d, $J = 19.6$ Hz), 114.4 (d, $J = 19.6$ Hz), 81.1 ppm. MS m/z for $\text{C}_{24}\text{H}_{20}\text{F}_2\text{N}_5\text{O}$, (ESI⁺) m/z : 432.2 [M + H]⁺. HRMS (ESI) m/z for $\text{C}_{24}\text{H}_{20}\text{F}_2\text{N}_5\text{O} = 432.1630$ [M + H]⁺, found 432.1632; elemental analysis calcd. (%) for $\text{C}_{24}\text{H}_{19}\text{F}_2\text{N}_5\text{O}$: C, 66.81; H, 4.44; F, 8.81; N, 16.23; O, 3.71; found: C, 66.82; H, 4.45; F, 8.81; N, 16.23; O, 3.70.

Compound 33b

$R_f = 0.49$ (Hex/EtOAc 2:1). ^1H NMR (400 MHz, CDCl_3) δ 7.72–7.68 (m, 1H), 7.63 (s, 1H), 7.47–7.43 (m, 1H), 7.39–7.37 (m, 1H), 7.31–7.26 (m, 4H), 7.18–7.16 (m, 2H), 7.06–7.02 (m, 4H), 6.43 (bs, 1H), 5.99 (s, 2H), 2.39 (s, 3H) ppm. ^{13}C (100 MHz, CDCl_3) δ 160.3, 156.7 (d, $J = 226.9$ Hz), 154.0, 140.1, 138.4, 136.2, 130.2, 128.6, 127.6, 127.1, 123.9, 123.5 (d, $J = 6.8$ Hz), 115.8 (d, $J = 22.4$ Hz), 82.5, 21.3 ppm. MS m/z for $\text{C}_{25}\text{H}_{22}\text{F}_2\text{N}_5$, (ESI⁺) m/z : 430.2 [M+H]⁺. HRMS (ESI) m/z for $\text{C}_{25}\text{H}_{22}\text{F}_2\text{N}_5 = 430.1838$ [M + H]⁺, found 430.1839; elemental analysis calcd. (%) for $\text{C}_{25}\text{H}_{21}\text{F}_2\text{N}_5$: C, 69.92; H, 4.93; F, 8.85; N, 16.31; found: C, 69.93; H, 4.94; F, 8.85; N, 16.31.

Procedure for the synthesis of disubstituted pyridine derivatives 35 and 36

In a microwave tube equipped with a stir bar, the monosubstituted pyridine **30** (1 equiv.) dissolved in anhydrous 1,4-dioxane (1.5 mL), morpholine (5 equiv.) and DIPEA (1.5 equiv.) were added. The reaction mixture was irradiated at 160 °C for 10h in a microwave oven. Then, the mixture was extracted with EtOAc, washed with brine, dried over anhydrous Na_2SO_4 and concentrated under vacuum. The crude was purified through column chromatography using PET/EtOAc 5:1 as eluant to give products **35** and **36** with 19 and 46% yield, respectively.

Compound 35

$R_f = 0.08$ (PET/EtOAc 5:1). ^1H NMR (400 MHz, CDCl_3) δ = 7.21 (m, 2H), 7.11 (m, 2H), 6.24 (d, $J = 1.6$ Hz, 1H), 6.0 (d, $J = 1.6$ Hz, 1H), 5.9 (s, 1H), 3.82–3.78 (m, 4H), 3.46 (t, $J = 4$ Hz, 2H), 3.25 (t, $J = 4$ Hz, 2H) ppm. ^{13}C (100 MHz, CDCl_3) δ 161.1, 157.6 (d, $J = 197.8$ Hz), 148.0, 134.8, 124.9 (d, $J = 6.6$ Hz), 124.6, 116.4 (d, $J = 22.6$ Hz), 100.0, 87.3, 68.8, 46.4 ppm. MS m/z for $\text{C}_{15}\text{H}_{16}\text{ClFN}_3\text{O}$, (ESI⁺) m/z : 308.1 [M + H]⁺.

Compound 36

$R_f = 0.37$ (PET/EtOAc 5:1). ^1H NMR (400 MHz, CDCl_3) δ 7.27 (m, 2H), 7.05 (t, $J = 8.8$ Hz, 2H), 6.24 (d, $J = 9.2$ Hz, 1H), 6.08 (d, $J = 4.8$ Hz, 1H), 3.81 (t, $J = 4.8$ Hz, 2H), 3.49 (t, $J = 4$ Hz, 2H) ppm. ^{13}C NMR (100 MHz, CDCl_3) δ 159.3, 159.1 (d, $J = 240.2$ Hz), 155.7, 146.4, 135.9, 123.4 (d, $J = 6.7$ Hz), 115.9 (d, $J = 22.4$ Hz), 97.4, 96.9, 66.7, 45.4 ppm. MS m/z for $\text{C}_{15}\text{H}_{16}\text{ClFN}_3\text{O}$, (ESI⁺) m/z : 308.1 [M + H]⁺.

Procedure for the synthesis of Boc-protected trisubstituted pyridine carbazate 37

In a microwave tube, compound **36** (1 equiv.), BocNHNH_2 (10 equiv.), $\text{Pd}_2(\text{dba})_3$ (0.04 equiv.), DPPF (0.12 equiv.), Cs_2CO_3 (2 equiv.) and dry toluene (1 mL) were added under an argon atmosphere. The reaction mixture was stirred at 150 °C for 10 min under microwave irradiation. The mixture was filtered through celite, rinsed with EtOAc and concentrated. The crude was purified using column chromatography with Hex/EtOAc 2:1 as eluant to give the product **37** with 42% yield.

$R_f = 0.38$ (Hex/EtOAc 2:1). ^1H NMR (400 MHz, CDCl_3) δ 7.31 (m, 2H), 7.0 (t, $J = 8.4$ Hz, 2H), 6.54 (s, 1H), 6.24 (s, 1H), 3.84 (t, $J = 4.8$ Hz, 2H), 3.51 (t, $J = 4.8$ Hz, 2H) ppm. ^{13}C (100 MHz, CDCl_3) δ 160.3, 159.6 (d, $J = 240.2$ Hz), 155.7, 154.2, 146.2, 135.8, 123.4 (d, $J = 6.8$ Hz), 115.9 (d, $J = 22.2$ Hz), 97.4, 96.8, 80.5, 66.9, 45.9, 28.3 ppm. MS m/z for $\text{C}_{20}\text{H}_{27}\text{FN}_5\text{O}_3$, (ESI⁺) m/z : 404.2 [M + H]⁺.

Procedure for the synthesis of trisubstituted pyridine derivatives 38a,b

Boc-protected pyridine **37** (1 equiv.) was dissolved in anhydrous CH_2Cl_2 (430 μL) and cooled to 0 °C. TFA (290 μL) was added, and the reaction mixture was warmed to 25 °C and stirred for 1h. After this time, the mixture was concentrated at reduced pressure. The residue obtained was pure enough to be subjected to the next step.

To a solution of hydrazine derivative (1 equiv.) in MeOH (10 mL), the opportune aldehyde (1 equiv.) and few drops of acetic acid were added. The mixture was stirred for 24 h at 25 °C and concentrated under vacuum. The residue was purified using column chromatography (Hex/EtOAc 1:1) furnishing the desired products **38a,b** with 37% and 33% yield, respectively.

Compound **38a**

$R_f = 0.31$ (Hex/EtOAc 1:1). $^1\text{H NMR}$ (400 MHz, CDCl_3) δ 10.63 (bs, 1H), 7.84 (s, 1H), 7.61 (bs, 1H), 7.46–7.36 (m, 2H), 7.30–7.27 (m, 3H), 7.17 (d, $J = 7.6$ Hz, 1H), 7.06–7.00 (m, 3H), 6.93 (t, d, $J = 7.6$ Hz 1H), 5.74–5.72 (m, 1H), 3.84–3.81 (m, 4H), 3.50–3.48 (m, 4H) ppm. ^{13}C (100 MHz, CDCl_3) δ 160.3, 156.7 (d, $J = 113.7$ Hz), 152.4, 142.5, 136.7, 130.7, 129.7, 125.0, 122.9, 122.8 (d, $J = 7.5$ Hz), 119.6, 118.0, 116.7, 116.4, 115.7 (d, $J = 22.3$ Hz), 81.8, 66.8, 45.7 ppm. MS m/z for $\text{C}_{22}\text{H}_{23}\text{FN}_5\text{O}_2$, (ESI⁺) m/z : 408.2 [M + H]⁺. HRMS (ESI) m/z for $\text{C}_{22}\text{H}_{23}\text{FN}_5\text{O}_2 = 408.1830$ [M + H]⁺, found 408.1831; elemental analysis calcd. (%) for $\text{C}_{22}\text{H}_{22}\text{FN}_5\text{O}_2$: C, 64.85; H, 5.44; F, 4.66; N, 17.19; O, 7.85; found: C, 64.83; H, 5.45; F, 4.66; N, 17.19; O, 7.86.

Compound **38b**

$R_f = 0.43$ (Hex/EtOAc 1:1). $^1\text{H NMR}$ (400 MHz, CDCl_3) δ 7.71 (bs, 1H), 7.65 (s, 1H), 7.44 (d, $J = 8.8$ Hz, 2H), 7.32–7.27 (m, 4H), 7.17 (d, $J = 7.6$ Hz, 1H), 7.05–7.01 (m, 2H), 5.91 (s, 2H), 3.85 (t, $J = 4.8$ Hz, 2H), 3.51 (t, $J = 4.8$ Hz, 2H), 2.42 (s, 3H) ppm. ^{13}C (100 MHz, CDCl_3) δ 162.5, 160.4, 158.1, 154.5, 138.4, 134.2, 130.3, 128.6, 127.3, 124.0, 123.9, 115.8 (d, $J = 22.3$ Hz), 81.9, 66.6, 46.4, 21.3 ppm. MS m/z for $\text{C}_{23}\text{H}_{25}\text{FN}_5\text{O}$, (ESI⁺) m/z : 406.2 [M + H]⁺. HRMS (ESI) m/z for $\text{C}_{23}\text{H}_{25}\text{FN}_5\text{O} = 406.2038$ [M + H]⁺, found 406.2036; elemental analysis calcd. (%) for $\text{C}_{23}\text{H}_{24}\text{FN}_5\text{O}$: C, 68.13; H, 5.97; F, 4.69; N, 17.27; O, 3.95; found: C, 68.11; H, 5.97; F, 4.69; N, 17.27; O, 3.96.

3.3. Biology—General Part

All solvents, reagents and human plasma were purchased from Sigma-Aldrich Srl (Milan, Italy). Milli-Q quality water (Millipore, Milford, MA, USA), acetonitrile (ACN) and formic acid (FA) were used for the chromatographic analyses. Cell culture mediums, fetal bovine serum (FBS), L-glutamine, and penicillin–streptomycin were purchased from Euroclone S.p.A. (Milan, Italy). SOF (MCE[®] cat. HY-15005), REM (MCE[®] cat. HY-104077) and RAL (MCE[®] cat. HY-10353), used as reference compounds, were purchased from MedChem Express (<https://www.medchemexpress.com>, accessed on 20 March 2024). RAL was dissolved in molecular grade water, and SOF and REM were dissolved in 100% dimethyl sulfoxide (DMSO).

3.4. Biology—Cells

3.4.1. Cell Culture

Cell-based assays were carried out on the normal human fibroblast FB789 cell line (kindly provided by Elena Dell’Ambra from IRCCS Istituto Dermopatico dell’Immacolata, Rome), on the Huh7 hepatocarcinoma cell line (kindly provided by Istituto Toscano Tumori, Core Research Laboratory, Siena, Italy), on the Caco-2 adenocarcinoma colorectal cell line (ATCC catalog. n. HTB-37), on the suspension H9 cell line (repository code ARP0001, NIBSC Centre for AIDS reagents) and on the adherent TZM-bl cell line (repository code ARP5011, NIBSC Centre for AIDS reagents).

The FB789 was cultured in Dulbecco’s Modified Eagle Medium (DMEM) and Ham’s F10 in a ratio of 50%, supplemented with 10% FBS, 2 mM L-glutamine, and 10,000 unit/mL penicillin/streptomycin.

Huh7 and Caco-2 were used to determine the cytotoxicity and the antiviral activity of candidate compounds against flaviviruses and SARS-CoV-2, respectively. H9 cells in combination with TZM-bl cells were used to evaluate the compounds against HIV-1, as described in the antiviral assays section.

High glucose Dulbecco’s Modified Eagle Medium with sodium pyruvate and L-glutamine (DMEM; Euroclone) was used to grow Huh-7 and TZM-bl. Minimum Es-

sential Eagle Medium (EMEM; Euroclone) was used to propagate Caco-2. DMEM and EMEM were supplemented with 10% fetal bovine serum (FBS; Euroclone) and 1% penicillin/streptomycin (Pen/Strep, Euroclone). The growth medium with a lower concentration of FBS (1%) was used for viral propagation, cytotoxic and antiviral experiments in adherent cell lines. Suspension cell lines were grown, propagated and infected in RPMI 1640 medium supplemented with 10% fetal bovine serum (FBS; Euroclone), 2 mM L-glutamine and 1% penicillin/streptomycin (Pen/Strep, Euroclone). All cell lines were grown at 37 °C in a 5% CO₂ atmosphere in a humidified incubator.

3.4.2. Cytotoxicity Assay

The cytotoxicity of all investigated compounds was assayed in all cells lines as previously described [12,13]. Briefly, confluent cells were treated with decreasing compound concentrations for 48h. The final DMSO concentration used was never greater than 0.5% *v/v*. Each experiment was performed in duplicate and repeated in two independent experiments. Cell viability was calculated using the CellTiter Glo 2.0 kit (Promega, Madison, WI, USA) and luminescence values signal obtained from cells treated with serial dilution of the compounds were measured through the GloMax[®] Discover Multi mode Microplate Reader (Promega) and elaborated with GraphPad PRISM software version 9.0 (La Jolla, San Diego, CA, USA). The half-maximal cytotoxic concentration (CC₅₀) was calculated using a non-linear regression analysis of the dose–response curves and the ECanything GraphPad function. A non-toxic dose of each compound was used as the starting concentration in the antiviral activity assay.

3.5. Biology—Viruses

3.5.1. Viruses

The New Guinea C DENV serotype 2 and the WNV lineage 1 (Italy/2009) strains were kindly provided by the Istituto Superiore di Sanità (Rome, Italy), while the SARS-CoV-2 strain belonging to lineage B.1 (EPI_ISL_2472896) was kindly provided by the Department of Biomedical and Clinical Sciences Luigi Sacco, University of Milan (Italy). Once expanded in VERO E6 (African green monkey kidney cell line, ATCC catalog. n. CRL-1586), DENV, WNV and SARS-CoV-2 viral stocks were stored at –80 °C and titrated as previously described [12,13]. HIV-1 wild-type reference strain NL4-3 (catalog. n. ARP2006) was obtained through the NIH AIDS Reagent Program and the viral titer was calculated in TZM-bl cells through the detection of β-galactosidase expression.

3.5.2. Antiviral Assays

Flaviviruses and SARS-CoV-2

To determine the antiviral activity of candidate compounds against DENV, WNV and SARS-CoV-2, a direct yield reduction assay based on the infection of cells in the presence of serial drug dilutions was performed as previously described with minor modifications [13]. Briefly, Huh7 or Caco-2 cells, pre-seeded in 96-well format, were infected with DENV and WNV viral stocks at 0.005 multiplicity of infection (MOI) or with SARS-CoV-2 at 0.004 MOI. After 1h of adsorption of the virus at 37 °C, viral inoculum was removed and serial dilutions of each tested compound, starting from the not-toxic dose, were added to the infected cells. After 48 h of incubation for DENV and WNV and 72 h for SARS-CoV-2, the antiviral activity was measured on the cell monolayer using immunodetection assay (IA), as previously described [13].

Absorbance was measured at 450 nm optical density (OD₄₅₀) using the Absorbance Module of the GloMax[®] Discover Multimode Microplate Reader (Promega). In each plate the suitable reference compound, a mock control (uninfected cells) and a virus control were included. Each IA run was validated when the OD₄₅₀ values of virus control showed an OD₄₅₀ > 1. All drug concentrations were tested in duplicate in two independent experiments. In each plate, SOF and REM were used as reference compounds against flaviviruses and SARS-CoV-2, respectively. Infected and uninfected cells without drugs

were used to calculate the 100% and the 0% of viral replication, respectively. The half-maximal inhibitory concentration (IC₅₀) was calculated through a non-linear regression analysis of the dose–response curves generated with GraphPad PRISM software version 9 (La Jolla, CA, USA). The Selectivity Index (SI) of the compounds was calculated as the ratio between the CC₅₀ and the IC₅₀.

HIV-1

The antiviral activity of investigated compounds was evaluated by measuring the IC₅₀ values against the HIV-1 wild-type reference strain NL4-3 in a TZM-bl cell line-based phenotypic assay named BiCycle Assay [14]. The method includes a first round of infection in H9 cells at 0.08 MOI in the presence of the serial dilution of compounds in a 96-well plate. In each plate the reference compound, the mock control (uninfected cells) and the virus control were included. After 72 h, 50 µl of supernatants from each well were used to infect the TZM-bl cell line, which allows the quantitative analysis of HIV-1 infection by measuring the expression of the luciferase gene integrated in the genome of the cells under the control of the HIV-1 LTR promoter. After 48 h, dose–response curves were generated by measuring reporter gene expression in each well by using Bright-Glo Luciferase Assay (Promega) through the GloMax[®] Discover Multimode Microplate Reader (Promega). Relative luminescence units measured in each well were elaborated with the GraphPad PRISM software version 9 to calculate IC₅₀ values.

3.6. In Vitro ADME

3.6.1. UV/LC-MS Method

For the quantitative analysis, a UV/LC-MS system was used. LC analysis was performed through an Agilent 1260 Infinity HPLC-DAD system (Agilent Technologies, Palo Alto, CA, USA), which constituted of a vacuum solvent degassing unit, a binary high-pressure gradient pump, and a UV detector, that was connected to an Agilent MSD 6130 system (Agilent Technologies, Palo Alto, CA, USA). The Agilent 1260 series mass spectra detection (MSD) single-quadrupole instrument was equipped with the orthogonal spray API-ES (Agilent Technologies, Palo Alto, CA, USA). Nitrogen was used as a nebulizing and drying gas. Chromatographic separation was performed using a Phenomenex Kinetex EVO C18-100 Å (150 × 4.6 mm, 5 µm particle size) at 25 °C and a gradient elution with a binary solution; eluent A was H₂O, while eluent B consisted of ACN (both eluents were acidified with FA 0.1% *v/v*). The analysis started with 0% of B for 1 min, then rapidly increased up to 80% of B in the 15 min remaining until 19 min; finally, in one minute, it returned to the initial conditions of 100% of A. The analysis was performed at a flow rate of 0.6 mL/min. UV detection was monitored at 254 nm. Spectra were acquired over the scan range *m/z* 100–1500 in positive mode.

3.6.2. Kinetic Aqueous Solubility

DMSO-stock compounds' solutions were diluted with Mill-Q H₂O to a final concentration of 200 µM. The percentage of DMSO never exceeded 2% *v/v*. Samples were incubated under gentle shaking at 25 °C (RT) conditions for 3 h. The suspensions were filtered using a 0.45 µm nylon filter (Acrodisc, VWR, Radnor, PE, USA), and the amount of solubilized compound was determined with the HPLC-UV-MS method reported above. The quantification of the solubilized compound was made with the appropriate calibration curve realized with stock solutions in DMSO (0.1–100 µg/mL). The limit of detection (LOD) was quantified at 0.1 µg/mL.

3.6.3. Parallel Artificial Membrane Permeability Assay (PAMPA)

To evaluate the apparent permeability of tested compounds, a DMSO stock solution [1 mM] of each derivative was prepared and then diluted 1:1 *v/v* with phosphate buffer (PBS 25 mM, pH 7.4) in order to make the donor solutions. According to the protocol already published [9,15], the gastrointestinal (GI) phospholipidic bilayer was mimed through

adding a 1% *w/v* dodecane solution of phosphatidylcholine (PC). The sandwich plates were assembled and incubated for 5 h at RT. At the end time point, the amount of compound passed through the phospholipid bilayer was measured using HPLC-UV/MS. Finally, apparent permeability (P_{app}) and membrane retention (MR%) were calculated as previously described [8].

3.6.4. Metabolic Stability Assay

A DMSO solution of selected compounds was incubated in the presence of phosphate buffer (25 mM, pH 7.4), human liver microsomal protein (200 $\mu\text{g}/\text{mL}$), and an NADPH regenerating system in MgCl_2 (48 mM) at a final concentration of 50 μM . The metabolic reactions were conducted for 1 h under shaking at 37 °C and then stopped by adding cold acetonitrile (ACN). Centrifuging the mixtures at 5000 rpm, the supernatant was separated, dried under nitrogen flow, and finally suspended in methanol (MeOH). The amount of the parent drug and the metabolites were determined as previously described [14].

3.6.5. Plasma Stability Assay

A DMSO solution of each compound was incubated at a final concentration of 100 μM at 37 °C under shaking with HEPES buffer (25 mM, 140 mM NaCl, pH 7.4) and human plasma. At time 0 and after 24 h, samples were collected from the reaction mixtures and treated with cold ACN. After centrifugation at 5000 rpm for 10 min, the supernatant was collected, and the amount of unmodified compound was determined using the HPLC-UV/MS method described above. Modified compounds were calculated using time zero as 100% of the unmodified compound.

4. Conclusions

In conclusion, two small libraries of derivatives containing pyrimidine and pyridine privileged scaffolds were synthesized using a scaffold morphing approach, starting from previously obtained triazines. Newly synthesized compounds have been evaluated for their anticancer activity on lymphoma, hepatocarcinoma, and colon epithelial carcinoma cells. Three pyrimidine derivatives, **19a**, **19b**, and **21a**, were the most potent compounds synthesized demonstrating CC_{50} values in the low micromolar range against Huh7 and Caco-1 cell lines coupled with a good selectivity, especially in the case of **19b**. Two pyridine compounds, **33b** and **38b**, were the most selective derivatives synthesized.

Finally, the above-mentioned five azines were evaluated with *in vitro* ADME protocols showing a generally suboptimal aqueous solubility accompanied by good passive permeability and discrete percentages of membrane retention. From the metabolic point of view, neither in presence of liver microsomes nor with human plasma, tested compounds underwent massive degradation, thus allowing us to state that most of them manage to reach the potential biological target unaltered. Further studies aimed at the identification of a specific biological target for the newly synthesized azines are ongoing in our laboratories.

Supplementary Materials: The following supporting information can be downloaded at: <https://www.mdpi.com/article/10.3390/molecules29071452/s1>, Supplement S1: Nuclear Overhauser Effect Spectroscopy (NOESY) of pyrimidine intermediates **11** and **12**; Supplement S2: ^1H NMR of pyridine intermediates **23** and **24**; Supplement S3: NMR spectra for highly decorated pyrimidines and pyridine derivatives.

Author Contributions: Conceptualization, L.B., M.Z. and E.D.; methodology, S.C., I.V., F.P. and S.F.; validation, E.M., L.F. and C.V.; formal analysis, E.D.M. and F.G.; investigation, B.M.B.; data curation, E.M., L.F., E.D.M., F.G., B.M.B. and C.V.; writing—original draft preparation, S.C., I.V., F.P. and S.F.; writing—review and editing, L.B., M.Z. and E.D.; supervision, R.S.; funding acquisition, R.S., E.D., M.Z. and L.B. All authors have read and agreed to the published version of the manuscript.

Funding: This research was funded by Ministero dell'Istruzione, dell'Università della Ricerca Italiano (MIUR), PRIN 2017, project N. 2017BMK8JR, Title "ORIGINALE CHEMIAE in Antiviral

Strategy—Origin and Modernization of Multi-Component Chemistry as a Source of Innovative Broad Spectrum Antiviral Strategy” (L.B., R.S., E.D. and M.Z.).

Institutional Review Board Statement: Not applicable.

Informed Consent Statement: Not Applicable.

Data Availability Statement: Data are contained within the article and Supplementary Materials.

Conflicts of Interest: M.Z. reports consultancy for ViiV Healthcare, Gilead Sciences, GlaxoSmithKline, Janssen-Cilag, Theratechnologies, Merck Sharp, and Dohme, and grants for his institution from ViiV Healthcare, Theratechnologies, and Gilead Sciences outside the submitted work. All other authors: no conflicts to declare.

References

1. Evans, B.E.; Rittle, K.E.; Bock, M.G.; DiPardo, R.M.; Freidinger, R.M.; Whitter, W.L.; Lundell, G.F.; Veber, D.F.; Anderson, P.S.; Chang, R.S.L.; et al. Methods for drug discovery: Development of potent, selective, orally effective cholecystokinin antagonists. *J. Med. Chem.* **1988**, *31*, 2235–2246. [[CrossRef](#)] [[PubMed](#)]
2. Kim, J.; Kim, H.; Park, S.B. Privileged structures: Efficient chemical “navigators” toward unexplored biologically relevant chemical spaces. *J. Am. Chem. Soc.* **2014**, *136*, 14629–14638. [[CrossRef](#)] [[PubMed](#)]
3. Kounde, C.S.; Yeo, H.Q.; Wang, Q.Y.; Wan, K.F.; Dong, H.; Karuna, R.; Dix, I.; Wagner, T.; Zou, B.; Simon, O.; et al. Discovery of 2-oxopiperazine dengue inhibitors by scaffold morphing of a phenotypic high-throughput screening hit. *Bioorg. Med. Chem. Lett.* **2017**, *27*, 1385–1389. [[CrossRef](#)] [[PubMed](#)]
4. Hu, Y.; Stumpfe, D.; Bajorath, J. Recent Advances in Scaffold Hopping. *J. Med. Chem.* **2017**, *60*, 1238–1246. [[CrossRef](#)] [[PubMed](#)]
5. Shah, D.R.; Modh, R.P.; Chikhaliya, K.H. Privileged s-triazines: Structure and pharmacological applications. *Future Med. Chem.* **2014**, *6*, 463–477. [[CrossRef](#)] [[PubMed](#)]
6. Josephitis, C.M.; Nguyen, H.M.; McNally, A. Late-Stage C–H Functionalization of Azines. *Chem. Rev.* **2023**, *123*, 7655–7691. [[CrossRef](#)] [[PubMed](#)]
7. Baumann, M.; Baxendale, I.R. An Overview of the Synthetic Routes to the Best Selling Drugs Containing 6-Membered Heterocycles. *Beilstein. J. Org. Chem.* **2013**, *9*, 2265–2319. [[CrossRef](#)] [[PubMed](#)]
8. Chiacchio, M.A.; Iannazzo, D.; Romeo, R.; Giofrè, S.V.; Legnani, L. Pyridine and Pyrimidine Derivatives as Privileged Scaffolds in Biologically Active Agents. *Curr. Med. Chem.* **2019**, *26*, 7166–7195. [[CrossRef](#)] [[PubMed](#)]
9. Cesarini, S.; Vicenti, I.; Poggialini, F.; Secchi, M.; Giammarino, F.; Varasi, I.; Lodola, C.; Zazzi, M.; Dreassi, E.; Maga, G.; et al. Privileged Scaffold Decoration for the Identification of the First Trisubstituted Triazine with Anti-SARS-CoV-2 Activity. *Molecules* **2022**, *27*, 8829. [[CrossRef](#)] [[PubMed](#)]
10. Pagani, G.A.; Abbotto, A. *Chimica Degli Eterocicli*, 1st ed.; Piccin: Padova, Italy, 1995; pp. 265–266.
11. Ono, M.; Zhang, S.; Przewloka, T.; Koya, K.; Kostik, E.; Wada, Y.; Sun, L.; Ying, W. Pyrimidine Compounds. U.S. Patent US6693097B2, 17 February 2004.
12. Ono, M.; Sun, L.; Wada, Y.; Przewloka, T.; Li, H.; Ng, H.P.; Demko, Z. Pyridine Compounds. U.S. Patent US7338951B2, 4 March 2008.
13. Vicenti, I.; Martina, M.G.; Boccuto, A.; De Angelis, M.; Giavarini, G.; Dragoni, F.; Marchi, S.; Trombetta, C.M.; Crespan, E.; Maga, G.; et al. System-oriented optimization of multi-target 2,6-diaminopurine derivatives: Easily accessible broad-spectrum antivirals active against flaviviruses, influenza virus and SARS-CoV-2. *Eur. J. Med. Chem.* **2021**, *224*, 113683. [[CrossRef](#)] [[PubMed](#)]
14. Sanna, C.; D’Abrosca, B.; Fiorentino, A.; Giammarino, F.; Vicenti, I.; Corona, A.; Caredda, A.; Tramontano, E.; Esposito, F. HIV-1 Integrase Inhibition Activity by Spiroketal Derivatives from *Plagius flosculosus*, an Endemic Plant of Sardinia (Italy) and Corsica (France). *Pharmaceuticals* **2023**, *16*, 1118. [[CrossRef](#)] [[PubMed](#)]
15. Poggialini, F.; Vagaggini, C.; Brai, A.; Pasqualini, C.; Crespan, E.; Maga, G.; Perini, C.; Cabella, N.; Botta, L.; Musumeci, F.; et al. Biological Evaluation and In Vitro Characterization of ADME Profile of In-House Pyrazolo[3,4-*d*]pyrimidines as Dual Tyrosine Kinase Inhibitors Active against Glioblastoma Multiforme. *Pharmaceutics* **2023**, *15*, 453. [[CrossRef](#)] [[PubMed](#)]

Disclaimer/Publisher’s Note: The statements, opinions and data contained in all publications are solely those of the individual author(s) and contributor(s) and not of MDPI and/or the editor(s). MDPI and/or the editor(s) disclaim responsibility for any injury to people or property resulting from any ideas, methods, instructions or products referred to in the content.